

This book distills the knowledge gained from research into atoms in molecules over the last 10 years into a unique, handy reference. Throughout, the authors address a wide audience, such that this volume may equally be used as a textbook without compromising its research-oriented character. Clearly structured, the text begins with advances in theory before moving on to theoretical studies of chemical bonding and reactivity. There follow separate sections on solid state and surfaces as well as experimental electron densities, before finishing with applications in biological sciences and drug-design.

The result is a must-have for physicochemists, chemists, physicists, spectroscopists and materials scientists.



Chérif F. Matta is an Assistant Professor of Chemistry at Mount Saint Vincent University and an Adjunct Professor of Chemistry at Dalhousie University, both in Halifax, Canada. He obtained his BSc from Alexandria University, Egypt, in 1987 and gained his PhD in theoretical chemistry from McMaster University, Hamilton, Canada in 2002. He was then a postdoctoral fellow at the University of Toronto, Canada, before being awarded an i. W. Killam Fellowship at Dalhousie University. Professor Matta has held the J. C. Polanyi Prize in Chemistry, two BioVision Next Fellowships, and a Chemistry Teaching Award, and has more than 40 papers and book chapters and two software programs to his credit. His research is in theoretical and computational chemistry with a focus on QTAIM and its applications.



Russell Boyd graduated from the University of British Columbia in chemistry in 1967, receiving his PhD in theoretical chemistry from McGill University in 1971. He subsequently went to Oxford University, UK, as a postdoctoral fellow, before returning to British Columbia with a Killam Postdoctoral Fellowship at the Department of Chemistry from 1973 to 1975. He then joined Dalhousie University, Halifax, where he held the Chair of Chemistry from 1992 to 2005 and became McLeod Chair in 2001. Professor Boyd has published about 200 papers in computational and theoretical chemistry. His current interests include the effects of radiation on DNA and proteins, the mechanism by which a leading anti-tumor drug cleaves DNA, and the design of catalysts.

Matta • Boyd

The Quantum Theory
of Atoms in Molecules

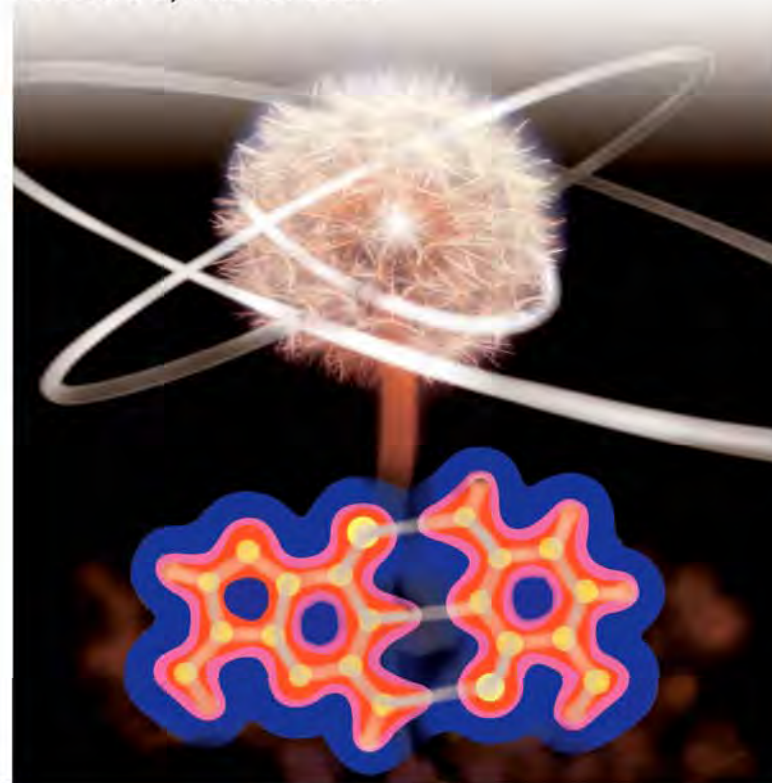
Edited by Chérif F. Matta
and Russell J. Boyd

WILEY-VCH

The Quantum Theory of Atoms in Molecules

From Solid State to DNA and Drug Design

Foreword by Axel D. Becke



BICENTENNIAL
1807
WILEY
2007
BICENTENNIAL

ISBN 978-3-527-30748-7



www.wiley-vch.de

WILEY-VCH

Contents

Foreword VII

Preface XIX

List of Abbreviations Appearing in this Volume XXVII

List of Contributors XXXIII

1 An Introduction to the Quantum Theory of Atoms in Molecules 1

Chérif F. Matta and Russell J. Boyd

- 1.1 Introduction 1
- 1.2 The Topology of the Electron Density 1
- 1.3 The Topology of the Electron Density Dictates the Form of Atoms in Molecules 5
- 1.4 The Bond and Virial Paths, and the Molecular and Virial Graphs 8
- 1.5 The Atomic Partitioning of Molecular Properties 9
- 1.6 The Nodal Surface in the Laplacian as the Reactive Surface of a Molecule 10
- 1.7 Bond Properties 10
 - 1.7.1 The Electron Density at the BCP (ρ_b) 11
 - 1.7.2 The Bonded Radius of an Atom (r_b), and the Bond Path Length 11
 - 1.7.3 The Laplacian of the Electron Density at the BCP ($\nabla^2\rho_b$) 11
 - 1.7.4 The Bond Ellipticity (ε) 12
 - 1.7.5 Energy Densities at the BCP 12
 - 1.7.6 Electron Delocalization between Bonded Atoms: A Direct Measure of Bond Order 13
- 1.8 Atomic Properties 15
 - 1.8.1 Atomic Electron Population [$N(\Omega)$] and Charge [$q(\Omega)$] 16
 - 1.8.2 Atomic Volume [$\text{Vol.}(\Omega)$] 16
 - 1.8.3 Kinetic Energy [$T(\Omega)$] 17
 - 1.8.4 Laplacian [$L(\Omega)$] 17
 - 1.8.5 Total Atomic Energy [$E_c(\Omega)$] 18

1.8.6	Atomic Dipolar Polarization [$\mu(\Omega)$]	20
1.8.7	Atomic Quadrupolar Polarization [$Q(\Omega)$]	24
1.9	“Practical” Uses and Utility of QTAIM Bond and Atomic Properties	25
1.9.1	The Use of QTAIM Bond Critical Point Properties	25
1.9.2	The Use of QTAIM Atomic Properties	26
1.10	Steps of a Typical QTAIM Calculation	27
	<i>References</i>	30

Part I Advances in Theory 35

2 The Lagrangian Approach to Chemistry 37

Richard F. W. Bader

2.1	Introduction	37
2.1.1	From Observation, to Physics, to QTAIM	37
2.2	The Lagrangian Approach	38
2.2.1	What is The Lagrangian Approach and What Does it Do?	38
2.2.2	The Lagrangian and the Action Principle – A Return to the Beginnings	39
2.2.3	Minimization of the Action	40
2.2.4	Steps in Minimizing the Action	41
2.3	The Action Principle in Quantum Mechanics	42
2.3.1	Schrödinger’s Appeal to the Action	42
2.3.2	Schrödinger’s Minimization	42
2.3.2.1	Two Ways of Expressing the Kinetic Energy	43
2.3.3	Obtaining an Atom from Schrödinger’s Variation	44
2.3.3.1	The Role of Laplacian in the Definition of an Atom	45
2.3.4	Getting Chemistry from $\delta G(\psi, \nabla\psi; \Omega)$	46
2.4	From Schrödinger to Schwinger	48
2.4.1	From Dirac to Feynman and Schwinger	48
2.4.2	From Schwinger to an Atom in a Molecule	49
2.5	Molecular Structure and Structural Stability	52
2.5.1	Definition of Molecular Structure	52
2.5.2	Prediction of Structural Stability	53
2.6	Reflections and the Future	53
2.6.1	Reflections	53
2.6.2	The Future	55
	<i>References</i>	57

3 Atomic Response Properties 61

Todd A. Keith

3.1	Introduction	61
3.2	Apparent Origin-dependence of Some Atomic Response Properties	62
3.3	Bond Contributions to “Null” Molecular Properties	64

3.4	Bond Contributions to Atomic Charges in Neutral Molecules	70
3.5	Atomic Contributions to Electric Dipole Moments of Neutral Molecules	71
3.6	Atomic Contributions to Electric Polarizabilities	73
3.7	Atomic Contributions to Vibrational Infrared Absorption Intensities	78
3.8	Atomic Nuclear Virial Energies	82
3.9	Atomic Contributions to Induced Electronic Magnetic Dipole Moments	88
3.10	Atomic Contributions to Magnetizabilities of Closed-Shell Molecules	90
	<i>References</i>	94
4	QTAIM Analysis of Raman Scattering Intensities: Insights into the Relationship Between Molecular Structure and Electronic Charge Flow	95
	<i>Kathleen M. Gough, Richard Dawes, Jason R. Dwyer, and Tammy L. Welshman</i>	
4.1	Introduction	95
4.2	Background to the Problem	96
4.2.1	Conceptual Approach to a Solution	97
4.2.1.1	Experimental Measurement of Raman Scattering Intensities	97
4.2.1.2	Theoretical Modeling of Raman Scattering Intensities: What We Did and Why	99
4.3	Methodology	100
4.3.1	Modeling α and $\partial\alpha/\partial r$	101
4.3.2	Recouping α From the Wavefunction, With QTAIM	102
4.3.3	Recovering $\partial\alpha/\partial r$ From QTAIM	103
4.4	Specific Examples of the Use of AIM2000 Software to Analyze Raman Intensities	103
4.4.1	Modeling α in H_2	104
4.4.1.1	Modeling $\Delta\bar{\alpha}/\Delta r$ in H_2	106
4.4.2	Modeling α and $\Delta\bar{\alpha}/\Delta r$ in CH_4	106
4.4.3	Additional Exercises for the Interested Reader	108
4.5	Patterns in α That Are Discovered Through QTAIM	109
4.6	Patterns in $\partial\alpha/\partial r_{CH}$ That Apply Across Different Structures, Conformations, Molecular Types: What is Transferable?	111
4.6.1	Patterns in $\Delta\bar{\alpha}/\Delta r_{CH}$ Revealed by QTAIM	111
4.6.1.1	QTAIM Analysis of $\Delta\bar{\alpha}/\Delta r_{CH}$ in Small Alkanes	111
4.6.1.2	What Did We Learn From QTAIM That Can be Transferred to the Other Molecules?	113
4.7	What Can We Deduce From Simple Inspection of $\partial\bar{\alpha}/\partial r_{CH}$ and $\partial\bar{\alpha}/\partial r_{CC}$ From Gaussian?	114
4.7.1	Variations in $\partial\bar{\alpha}/\partial r_{CH}$ Among the Alkanes	114
4.7.2	$\Delta\bar{\alpha}/\Delta r_{CH}$ in Cycloalkanes, Bicycloalkanes, and Hedranes	116
4.7.3	Patterns That Emerge in $\Delta\bar{\alpha}/\Delta r_{CC}$ of Alkanes	116

4.7.4	Unsaturated Hydrocarbons and the Silanes: C–H, C=C, and Si–Si Derivatives	117
4.8	Conclusion	118
	<i>References</i>	119
5	Topological Atom–Atom Partitioning of Molecular Exchange Energy and its Multipolar Convergence	121
	<i>Michel Rafat and Paul L. A. Popelier</i>	
5.1	Introduction	121
5.2	Theoretical Background	123
5.3	Details of Calculations	128
5.4	Results and Discussion	130
5.4.1	Convergence of the Exchange Energy	130
5.4.2	Convergence of the Exchange Force	136
5.4.3	Diagonalization of a Matrix of Exchange Moments	136
5.5	Conclusion	139
	<i>References</i>	139
6	The ELF Topological Analysis Contribution to Conceptual Chemistry and Phenomenological Models	141
	<i>Bernard Silvi and Ronald J. Gillespie</i>	
6.1	Introduction	141
6.2	Why ELF and What is ELF?	142
6.3	Concepts from the ELF Topology	144
6.3.1	The Synaptic Order	145
6.3.2	The Localization Domains	145
6.3.3	ELF Population Analysis	147
6.4	VSEPR Electron Domains and the Volume of ELF Basins	149
6.5	Examples of the Correspondence Between ELF Basins and the Domains of the VSEPR Model	153
6.5.1	Octet Molecules	153
6.5.1.1	Hydrides (CH ₄ , NH ₃ , H ₂ O)	153
6.5.1.2	AX ₄ (CH ₄ , CF ₄ , SiCl ₄)	154
6.5.1.3	AX ₃ E and AX ₂ E ₂ (NCl ₃ , OCl ₂)	154
6.5.2	Hypervalent Molecules	155
6.5.2.1	PCl ₅ and SF ₆	155
6.5.2.2	SF ₄ and ClF ₃	155
6.5.2.3	AX ₇ and AX ₆ E Molecules	155
6.5.3	Multiple Bonds	156
6.5.3.1	C ₂ H ₄ and C ₂ H ₂	156
6.5.3.2	Si ₂ Me ₄ and Si ₂ Me ₂	157
6.6	Conclusions	158
	<i>References</i>	159

Part II	Solid State and Surfaces	163
7	Solid State Applications of QTAIM and the Source Function – Molecular Crystals, Surfaces, Host–Guest Systems and Molecular Complexes	165
	<i>Carlo Gatti</i>	
7.1	Introduction	165
7.2	QTAIM Applied to Solids – the TOPOND Package	166
7.2.1	QTAIM Applied to Experimental Densities: TOPXD and XD Packages	168
7.3	QTAIM Applied to Molecular Crystals	170
7.3.1	Urea	171
7.3.1.1	Urea: Packing Effects	172
7.4	QTAIM Applied to Surfaces	179
7.4.1	Si(111)(1 × 1) Clean and Hydrogen-covered Surfaces	180
7.4.2	Si(111)(2 × 1) Reconstructed Surface	184
7.5	QTAIM Applied to Host–Guest Systems	186
7.5.1	Type I Inorganic Clathrates A ₈ Ga ₁₆ Ge ₃₀ (A = Sr, Ba)	186
7.5.2	Sodium Electrosodalite	190
7.6	The Source Function: Theory	192
7.6.1	The Source Function and Chemical Transferability	194
7.6.2	Chemical Information from the Source Function: Long and Short-range Bonding Effects in Molecular Complexes	196
7.6.3	The Source Function: Latest Developments	201
	<i>References</i>	202
8	Topology and Properties of the Electron Density in Solids	207
	<i>Víctor Luaña, Miguel A. Blanco, Aurora Costales, Paula Mori-Sánchez, and Angel Martín Pendás</i>	
8.1	Introduction	207
8.2	The Electron Density Topology and the Atomic Basin Shape	209
8.3	Crystalline Isostructural Families and Topological Polymorphism	213
8.4	Topological Classification of Crystals	215
8.5	Bond Properties – Continuity from the Molecular to the Crystalline Regime	217
8.6	Basin Partition of the Thermodynamic Properties	219
8.7	Obtaining the Electron Density of Crystals	222
	<i>References</i>	227
9	Atoms in Molecules Theory for Exploring the Nature of the Active Sites on Surfaces	231
	<i>Yosslen Aray, Jesus Rodríguez, and David Vega</i>	
9.1	Introduction	231
9.2	Implementing the Determination of the Topological Properties of $\rho(\mathbf{r})$ from a Three-dimensional Grid	231

- 9.3 An Application to Nanocatalysts – Exploring the Structure of the Hydrodesulfurization MoS₂ Catalysts 236
 - 9.3.1 Catalyst Models 237
 - 9.3.2 The Full $\rho(r)$ Topology of the MoS₂ Bulk 241
 - 9.3.3 The $\rho(r)$ Topology of the MoS₂ Edges 245
- References* 254

Part III Experimental Electron Densities and Biological Molecules 257

10 Interpretation of Experimental Electron Densities by Combination of the QTAMC and DFT 259

Vladimir G. Tsirelson

- 10.1 Introduction 259
- 10.2 Specificity of the Experimental Electron Density 261
- 10.3 Approximate Electronic Energy Densities 262
 - 10.3.1 Kinetic and Potential Energy Densities 262
 - 10.3.2 Exchange and Correlation Energy Densities 271
- 10.4 The Integrated Energy Quantities 275
- 10.5 Concluding Remarks 276
- References* 278

11 Topological Analysis of Proteins as Derived from Medium and High-resolution Electron Density: Applications to Electrostatic Properties 285

Laurence Leherste, Benoît Guillot, Daniel P. Vercauteren, Virginie Pichon-Pesme, Christian Jelsch, Angélique Lagoutte, and Claude Lecomte

- 11.1 Introduction 285
- 11.2 Methodology and Technical Details 287
 - 11.2.1 Ultra-high X-ray Resolution Approach 287
 - 11.2.2 Medium-resolution Approach 289
 - 11.2.2.1 Promolecular Electron Density Distribution Calculated from Structure Factors 289
 - 11.2.2.2 Promolecular Electron Density Distribution Calculated from Atoms 290
 - 11.2.3 A Test System – Human Aldose Reductase 291
- 11.3 Topological Properties of Multipolar Electron Density Database 294
- 11.4 Analysis of Local Maxima in Experimental and Promolecular Medium-resolution Electron Density Distributions 298
 - 11.4.1 Experimental and Promolecular Electron Density Distributions Calculated from Structure Factors 299
 - 11.4.2 Promolecular Electron Density Distributions Calculated from Atoms (PASA Model) 301
- 11.5 Calculation of Electrostatic Properties from Atomic and Fragment Representations of Human Aldose Reductase 305
 - 11.5.1 Medium- and High-resolution Approaches of Electrostatic Potential Computations 307

11.5.2	Electrostatic Potential Comparisons	309
11.5.3	Electrostatic Interaction Energies	312
11.6	Conclusions and Perspectives	312
	<i>References</i>	314
12	Fragment Transferability Studied Theoretically and Experimentally with QTAIM – Implications for Electron Density and Invariom Modeling	317
	<i>Peter Luger and Birger Dittrich</i>	
12.1	Introduction	317
12.2	Experimental Electron-density Studies	318
12.2.1	Experimental Requirements	318
12.2.2	Recent Experimental Advances	319
12.2.2.1	Synchrotron Radiation Compared with Laboratory Sources	319
12.2.2.2	Data Collection at Ultra-low Temperatures (10–20 K)	321
12.3	Studying Transferability with QTAIM – Atomic and Bond Topological Properties of Amino Acids and Oligopeptides	323
12.4	Invariom Modeling	328
12.4.1	Invariom Notation, Choice of Model Compounds, and Practical Considerations	330
12.4.2	Support for Pseudoatom Fragments from QTAIM	331
12.5	Applications of Aspherical Invariom Scattering Factors	334
12.5.1	Molecular Geometry and Anisotropic Displacement Properties	334
12.5.2	Using the Enhanced Multipole Model Anomalous Dispersion Signal	335
12.5.3	Modeling the Electron Density of Oligopeptide and Protein Molecules	336
12.6	Conclusion	338
	<i>References</i>	339
Part IV	Chemical Bonding and Reactivity	343
13	Interactions Involving Metals – From “Chemical Categories” to QTAIM, and Backwards	345
	<i>Piero Macchi and Angelo Sironi</i>	
13.1	Introduction	345
13.2	The Electron Density in Isolated Metal Atoms – Hints of Anomalies	345
13.3	Two-center Bonding	349
13.3.1	The Dative Bond	350
13.3.1.1	Metal Carbonyls	351
13.3.1.2	Donor–Acceptor Interactions of Heavy Elements	352
13.3.2	Direct Metal–Metal Bonding	352
13.4	Three-center Bonding	356
13.4.1	π -Complexes	357
13.4.2	σ -Complexes	363

- 13.4.2.1 Dihydrogen and Dihydride Coordination 364
- 13.4.2.2 Agostic Interactions 364
- 13.4.2.3 Hydride Bridges 367
- 13.4.3 Carbonyl-supported Metal–Metal Interactions 370
- 13.5 Concluding Remarks 371
 - References* 372

- 14 Applications of the Quantum Theory of Atoms in Molecules in Organic Chemistry – Charge Distribution, Conformational Analysis and Molecular Interactions 375**
 - Jesús Hernández-Trujillo, Fernando Cortés-Guzmán, and Gabriel Cuevas*

 - 14.1 Introduction 375
 - 14.2 Electron Delocalization 375
 - 14.2.1 The Pair-density 375
 - 14.2.2 $^3J_{\text{HH}}$ Coupling Constants and Electron Delocalization 378
 - 14.3 Conformational Equilibria 380
 - 14.3.1 Rotational barriers 380
 - 14.3.1.1 Rotational Barrier of Ethane 380
 - 14.3.1.2 Rotational Barrier of 1,2-Disubstituted Ethanes 382
 - 14.3.2 Anomeric Effect on Heterocyclohexanes 386
 - 14.4 Aromatic Molecules 391
 - 14.4.1 Electronic Structure of Polybenzenoid Hydrocarbons 391
 - 14.5 Conclusions 395
 - References* 396

- 15 Aromaticity Analysis by Means of the Quantum Theory of Atoms in Molecules 399**
 - Eduard Matito, Jordi Poater, and Miquel Solà*

 - 15.1 Introduction 399
 - 15.2 The Fermi Hole and the Delocalization Index 401
 - 15.3 Electron Delocalization in Aromatic Systems 403
 - 15.4 Aromaticity Electronic Criteria Based on QTAIM 404
 - 15.4.1 The *para*-Delocalization Index (PDI) 404
 - 15.4.2 The Aromatic Fluctuation Index (FLU) 406
 - 15.4.3 The π -Fluctuation Aromatic Index (FLU $_{\pi}$) 407
 - 15.5 Applications of QTAIM to Aromaticity Analysis 409
 - 15.5.1 Aromaticity of Buckybowls and Fullerenes 409
 - 15.5.2 Effect of Substituents on Aromaticity 412
 - 15.5.3 Assessment of Clar's Aromatic π -Sextet Rule 416
 - 15.5.4 Aromaticity Along the Diels–Alder Reaction. The Failure of Some Aromaticity Indexes 418
 - 15.6 Conclusions 419
 - References* 421

16	Topological Properties of the Electron Distribution in Hydrogen-bonded Systems	425
	<i>Ignasi Mata, Ibon Alkorta, Enrique Espinosa, Elies Molins, and José Elguero</i>	
16.1	Introduction	425
16.2	Topological Properties of the Hydrogen Bond	426
16.2.1	Topological Properties at the Bond Critical Point (BCP)	426
16.2.2	Integrated Properties	429
16.3	Energy Properties at the Bond Critical Point (BCP)	431
16.4	Topological Properties and Interaction Energy	435
16.5	Electron Localization Function, $\eta(r)$	438
16.6	Complete Interaction Range	440
16.6.1	Dependence of Topological and Energy Properties on the Interaction Distance	440
16.6.2	Perturbed Systems	448
16.7	Concluding Remarks	450
	<i>References</i>	450
17	Relationships between QTAIM and the Decomposition of the Interaction Energy – Comparison of Different Kinds of Hydrogen Bond	453
	<i>Śławomir J. Grabowski</i>	
17.1	Introduction	453
17.2	Diversity of Hydrogen-bonding Interactions	456
17.3	The Decomposition of the Interaction Energy	459
17.4	Relationships between the Topological and Energy Properties of Hydrogen Bonds	460
17.5	Various Other Interactions Related to Hydrogen Bonds	464
17.5.1	$H^+ \cdots \pi$ Interactions	464
17.5.2	Hydride Bonds	466
17.6	Summary	467
	<i>References</i>	468
Part V	Application to Biological Sciences and Drug Design	471
18	QTAIM in Drug Discovery and Protein Modeling	473
	<i>Nagamani Sukumar and Curt M. Breneman</i>	
18.1	QSAR and Drug Discovery	473
18.2	Electron Density as the Basic Variable	474
18.3	Atom Typing Scheme and Generation of the Transferable Atom Equivalent (TAE) Library	476
18.4	TAE Reconstruction and Descriptor Generation	478
18.5	QTAIM-based Descriptors	480
18.5.1	TAE Descriptors	482
18.5.2	RECON Autocorrelation Descriptors	485
18.5.3	PEST Shape–Property Hybrid Descriptors	485

18.5.4	Electron Density-based Molecular Similarity Analysis	487
18.6	Sample Applications	489
18.6.1	QSAR/QSPR with TAE Descriptors	489
18.6.2	Protein Modeling with TAE Descriptors	491
18.7	Conclusions	492
	<i>References</i>	494
19	Fleshing-out Pharmacophores with Volume Rendering of the Laplacian of the Charge Density and Hyperwall Visualization Technology	499
	<i>Preston J. MacDougall and Christopher E. Henze</i>	
19.1	Introduction	499
19.2	Computational and Visualization Methods	501
19.2.1	Computational Details	501
19.2.2	Volume Rendering of the Laplacian of the Charge Density	501
19.2.3	The Hyperwall	505
19.2.4	Hyper-interactive Molecular Visualization	505
19.3	Subatomic Pharmacophore Insights	507
19.3.1	Hydrogen-bonding Donor Sites	507
19.3.2	Inner-valence Shell Charge Concentration (i-VSCC) Features in Transition-metal Atoms	509
19.3.3	Misdirected Valence in the Ligand Sphere of Transition-metal Complexes	511
19.4	Conclusion	513
	<i>References</i>	514
	Index	515

Preface

“The manner in which the electron density is disposed in a molecule has not received the attention its importance would seem to merit. Unlike the energy of a molecular system which requires a knowledge of the second-order density matrix for its evaluation [a] many of the observable properties of a molecule are determined in whole or in part by the simple three-dimensional electron-density distribution. In fact, these properties provide a direct measure of a wide spectrum of different moments averaged directly over the density distribution. Thus the diamagnetic susceptibility, the dipole moment, the diamagnetic contribution to the nuclear screening constant, the electric field, and the electric field gradient (as obtained from nuclear quadrupole coupling constants) provide a measure of (aside from any angular dependencies) $\langle r_i^2 \rangle$, $\langle r_i \rangle$, $\langle r_i^{-1} \rangle$, $\langle r_i^{-2} \rangle$, and $\langle r_i^{-3} \rangle$, respectively. The electric field at a nucleus due to the electron density distribution is of particular interest due to the theorem derived by Hellmann [b] and Feynman [c]. They have demonstrated that the force acting on a nucleus in a molecule is determined by the electric field at that nucleus due to the other nuclei and to the electron-density distribution.”

- a P.-O. Löwdin, *Adv. Chem. Phys.* **2**, 207 (1959)
- b J. Hellman, *Einführung in die Quantenchemie* (Detliche, Leipzig, Germany, 1937)
- c R.P. Feynman, *Phys. Rev.* **56**, 340 (1939)

Richard F.W. Bader and Glenys A. Jones (1963) [a]

It has been sixteen years since the publication of Richard Bader’s classic 1990 treatise “*Atoms in Molecules: A Quantum Theory*” [b]. The theory was founded on the recognition that the electron density plays a critical role in explaining and understanding the experimental observations of chemistry. Bader’s work is among the earliest to draw attention to the importance of the electron density in chemistry, as the opening quotation, predating the discovery of the Hohenberg–Kohn

theorem, suggests. This 1963 paper includes an early example of molecular electron density contour plots (of the ammonia molecule).

Bader's fundamental work in the sixties on molecular electron density distributions (Table 1) laid the foundations for the theory which was developed in the seventies and eighties by his research group, which became known as the theory of atoms in molecules (AIM). In more recent literature this theory is often called the quantum theory of atoms in molecules (QTAIM) in recognition of its rigorous basis in quantum mechanics [2–6]. The theory relates the concepts of chemistry, for example chemical structure, chemical bonding, transferability of functional groups, and chemical reactivity, to the topology of the underlying electron-density distribution(s). QTAIM has, in effect, moved theoretical chemistry into real three-dimensional space [7]. In Bader's words:

“the charge [electron] density provides a description of the distribution of charge throughout real space and is the bridge between the concept of state functions in Hilbert space and the physical model of matter in real space.” [2]

By defining “proper open quantum systems” as special bounded regions within a closed (whole) system, followed by the identification of these regions as “atoms in molecules”, the quantum theory of atoms in molecules brought quantum mechanics into applicability to an atom *within* a molecule. When a molecular property can be expressed in terms of a property *density*, the contribution of an atom to that molecular property can be obtained by integrating this density over the bounded volume of that atom in the molecule. In this way every atom in a molecule or crystal is characterized by a set of physical properties, each of which corresponds to a molecular property. These atomic properties, naturally, add up to those of the total molecular system and, for this reason, parallel and recover the properties of the atoms of experimental chemistry [8]. In this sense, the quantum theory of atoms in molecules is *the* quantum mechanics of atoms within molecules and crystals [9–11].

The virial theorem, which governs the relationship between the potential and kinetic energies of a molecule, occupies a prominent place in molecular quantum mechanics. This theorem has been generalized by Bader from its *global* statement (which applies to the molecule as a whole) to a *local* statement defined at every point in space [10]. In other words, the theorem has been re-written in its most general form which applies at every point of space in terms of scalar functions of space, i.e. densities. This very important generalization, known as the “local statement of the virial theorem”, Eq. (54) in Ref. [10] and Eq. (10) in Chapter 1, is, perhaps, and to the best of our knowledge, the *only* known local relationship between the energy densities and the electron density that applies everywhere in space. More precisely, the local virial theorem relates the potential energy density and the kinetic energy density distributions locally to a function of the electron density, namely, its Laplacian [2, 10]. Bader also postulated [12], and later showed [2, 13–15] that the integrated form of this theorem, discovered before its local expression, translates into a virial theorem satisfied by each atom within a molecule

Table 1 Early Publications (nineteen-sixties) on molecular electron density distributions by Professor Richard F.W. Bader.

-
1. R.F.W. Bader and G.A. Jones, "The Hellmann-Feynman Theorem and Chemical Binding", *Canadian Journal of Chemistry*, **39**, (1961), 1253–1265.
 - 2.* R.F.W. Bader, "Vibrationally Induced Perturbations in Molecular Electron Distributions", *Canadian Journal of Chemistry*, **40**, (1962), 1164–1175.
 3. R.F.W. Bader and G.A. Jones, "The Electron Density Distributions in Hydride Molecules, I, The Water Molecule", *Canadian Journal of Chemistry*, **41**, (1963), 586–606.
 4. R.F.W. Bader and G.A. Jones, "The Electron Density Distribution in Hydride Molecules, II, The Ammonia Molecule", *Journal of Chemical Physics*, **38**, (1963), 2791–2802.
 5. R.F.W. Bader and G.A. Jones, "The Electron Density Distributions in Hydride Molecules, III, The Hydrogen Fluoride Molecule", *Canadian Journal of Chemistry*, **41**, (1963), 2251–2264.
 6. R.F.W. Bader, "Binding Regions in Polyatomic Molecules and Electron Density Distributions", *Journal of the American Chemical Society*, **86**, (1964), 5070–5075.
 7. R.F.W. Bader, W.H. Henneker and P.E. Cade, "Molecular Charge Distributions and Chemical Binding", *Journal of Chemical Physics*, **46**, (1967), 3341–3363.
 8. R.F.W. Bader, I. Keaveny and P.E. Cade, "Molecular Charge Distributions and Chemical Binding II. First-Row Diatomic Hydrides", *Journal of Chemical Physics*, **47**, (1967), 3381–3402.
 9. R.F.W. Bader and A.K. Chandra, "A View of Bond Formation in Terms of Molecular Charge Distributions", *Canadian Journal of Chemistry*, **46**, (1968), 953–966.
 10. R.F.W. Bader and A.D. Bandrauk, "Molecular Charge Distributions and Chemical Binding III. The Isoelectronic Series N₂, CO, BF and C₂, BeO, LiF", *Journal of Chemical Physics*, **49**, (1968), 1653–1665.
 11. R.F.W. Bader and A.D. Bandrauk, "Relaxation of the Molecular Charge Distribution and the Vibrational Force Constant", *Journal of Chemical Physics*, **49**, (1968), 1666–1675.
 12. R.F.W. Bader and H.J.T. Preston, "The Kinetic Energy of Molecular Charge Distributions and Molecular Stability", *International Journal of Quantum Chemistry*, **3**, (1969), 327–347.
 13. R.F.W. Bader, I. Keaveny and G. Runtz, "Polarizations of Atomic and Molecular Charge Distributions", *Canadian Journal of Chemistry*, **47**, (1969), 2308–2311.
 14. R.F.W. Bader, P.E. Cade, W.H. Henneker and I. Keaveny, "Molecular Charge Distributions and Chemical Binding IV. The Second-Row Diatomic Hydrides, AH", *Journal of Chemical Physics*, **50**, (1969), 5313–5333.
 15. R.F.W. Bader and J.L. Ginsburg, "Relaxations of Molecular Charge Distributions and the Vibrational Force Constants in Diatomic Hydrides", *Canadian Journal of Chemistry*, **47**, (1969), 3061–3074.
-

*This paper presents an early formulation of the symmetry rules predicting the outcome of unimolecular and bimolecular reactions. Kenichi Fukui describes this paper as "the important theory of Bader" in his 1981 Nobel Lecture in the paragraph he devotes to "names which are worthy of special mention".

or an extended system (Eq. (33) of Chapter 1). This result, termed the “atomic virial theorem”, in its turn led to the definition of the energy of an atom within a larger system, for example a molecule or a crystal, i.e. an “atomic energy”. The energy of an atom in a molecule, a very desirable quantity, remained totally elusive until the discovery of the atomic virial theorem, because this energy must, for example, include contributions from the nuclear–nuclear repulsion energy, contributions which are not trivial to partition on an atom-by-atom basis (Chapters 1 and 3).

Bader’s early studies of molecular electron density distributions (Table 1) coincided with the ground-breaking formulation of modern density functional theory (DFT) [16] in 1964 and 1965 by Walter Kohn and his co-workers [17, 18]. Contemporary DFT functionals (for example those developed by Axel Becke [19–22], and Lee et al. [23]) are capable of achieving chemical accuracy and of producing electron-density maps of unprecedented quality, and rapidly.

The advent of DFT, the spectacular increase in the power of computers, and algorithmic advances all led to an explosive growth in the number of studies applying the quantum theory of atoms in molecules to a very wide range of problems (as will be seen in this book) from solid-state physics; to the science of materials; to surface science; to X-ray analyses; to organic, physical–organic, organometallic, and inorganic chemistry; and to biochemistry and drug design. Accurate calculated (and experimental) electron-density maps of larger and larger systems are now routinely computed and analyzed using the QTAIM.

The theory has also benefited significantly from parallel advances in accurate X-ray crystallography. The development of multipolar refinement techniques, pioneered by Hansen and Coppens [24–26], coupled with low-temperature data collection and ever-more sensitive CCD detectors, has enabled crystallographers, for the first time, to obtain high-resolution experimental electron-density maps of quality sufficient to capture the fine details of the electron density in the bonding regions between atoms. Nowadays, crystallographers rely routinely on QTAIM to decode the wealth of chemical information contained in accurate experimental electron-density maps, bringing crystallography and chemical theory closer than ever before (see, for example, Refs [25–28] and the literature cited therein).

Bader’s landmark book [2], which includes (but is more than) an authoritative review of the theory up to 1990, sets forth the development and principles of this theory and explains how the atoms of experiment arise naturally from the laws of quantum mechanics. Since 1990 the field of QTAIM has grown dramatically both conceptually and in terms of the volume of publications and citations, a growth that has been reflected in several reviews (see, for example, Refs [3–6, 25–30]). In 1996, a special issue of the *Canadian Journal of Chemistry* was dedicated to Richard Bader on the occasion of his 65th birthday [31]. The objective of this book is to cover the developments in this field since the publication of Bader’s book.

QTAIM is rigorous, beautiful, and powerful. It provides a unifying thread of physical insight in chemistry, which explains its popularity. The breadth of QTAIM and its applications renders a comprehensive treatment of all its ramifi-

cations impossible in a book of this size. We have therefore *sampled* research in QTAIM by extending invitations to a necessarily incomplete group of world-leading researchers to review their respective contributions to the field. This has resulted in a volume written by fifty authors representing thirteen countries in five different continents (a list of contributors is given below). Despite this impressive list of contributors, we could not possibly have invited all the leaders of the field, unavoidable omissions for which we do apologize. These omissions, however, do not diminish the value of the phenomenal cross-section and depth of current fundamental and applied research in QTAIM that has been captured in this book.

As the editors of this book it is with considerable humility that we start with our own introductory chapter. The *only* reason for this choice is to facilitate the reading of the remainder of the book by introducing the basic concepts and terminology. The order of the other parts and chapters is purely and exclusively based on what we think is their logical order. All chapters, including our own, have been carefully refereed by at least three independent reviewers and were all revised and corrected before final acceptance.

The book is divided into five parts. The introductory chapter is followed by Part II which concentrates on the fundamental advances in the theory itself. Part II reviews the rapid development in the applications of the QTAIM to periodic systems (solid state and surfaces). Part III focuses on developments resulting from the synergy between experimental highly accurate X-ray crystallography and the QTAIM, with particular emphasis on the electron density of large biological molecules. Part VI deals with the wide diversity of applications of the QTAIM in organic, physical organic, and organometallic chemistry, and reviews the characterization of conventional and non-conventional chemical bonding. Part V reports on important developments in the use of QTAIM in the modeling of biological molecules and drug design.

We would like to thank each one of the authors individually for his or her invaluable contribution to this volume, and we thank Professor Axel D. Becke for writing the Foreword. We are much indebted to our publisher, Wiley-VCH, and its staff for their continual support, professionalism, and invaluable help, with special thanks to Nele Denzau, Dr. Tim Kersebohm, Dr. Romy Kirsten, Claudia Nussbeck, Dr. Martin Ottmar, Dr. Gudrun Walter, and Dr. Waltraud Wüst. We are particularly grateful for the care, rigor, and effort of our peer-reviewers (many of whom are also among the authors of chapters in this book): Professor Richard F.W. Bader, Dr. Miguel Blanco, Professor Curt M. Breneman, Dr. Clémence Corminboeuf, Professor Katherine V. Darvesh, Dr. Jason R. Dwyer, Dr. Carlo Gatti, Professor Kathleen M. Gough, Professor Sławomir J. Grabowski, Professor George L. Heard, Professor Jesús Hernández-Trujillo, Dr. Sian T. Howard, Professor Claude Lecomte, Professor Victor Luaña, Professor Peter Luger, Dr. Piero Macchi, Professor Preston J. MacDougall, Professor Louis J. Massa, Professor Angel Martín Pendás, Dr. James A. Platts, Dr. Paul L.A. Popelier, Dr. Kathy N. Robertson, Professor Bernard Silvi, Professor Vladimir G. Tsirelson, and Dr. Elizabeth A. Zhurova – we thank them all.

It is with delight that we dedicate this work to Professor Richard F.W. Bader on the occasion of his 75th birthday.

Halifax, October 2006

Chérif F. Matta and Russell J. Boyd

References

- 1 R.F.W. Bader, G.A. Jones; The electron density distribution in hydride molecules. The ammonia molecule. *J. Chem. Phys.* **1963**, 38, 2791–2802.
- 2 R.F.W. Bader; *Atoms in Molecules: A Quantum Theory*; Oxford University Press: Oxford, U.K., 1990.
- 3 R.F.W. Bader; The quantum mechanical basis of conceptual chemistry. *Monatsh. Chem.* **2005**, 136, 819–854.
- 4 R.F.W. Bader; 1997 Polanyi Award Lecture: Why are there atoms in chemistry? *Can. J. Chem.* **1998**, 76, 973–988.
- 5 R.F.W. Bader, in: P.v.-R. Schleyer (Ed.); *Encyclopedia of Computational Chemistry*; John Wiley and Sons: Chichester, UK, 1998, pp 64–86.
- 6 P.L.A. Popelier; *Atoms in Molecules: An Introduction*; Prentice Hall: London, 2000.
- 7 R.F.W. Bader, P.L.A. Popelier, T.A. Keith; Theoretical definition of a functional group and the molecular orbital paradigm. *Angew. Chem. Int. Ed. Engl.* **1994**, 33, 620–631.
- 8 C.F. Matta, R.F.W. Bader; An experimentalist's reply to "What is an atom in a molecule?"; *J. Phys. Chem. A* **2006**, 110, 6365–6371.
- 9 R.F.W. Bader; Principle of stationary action and the definition of a proper open system. *Phys. Rev. B* **1994**, 49, 13348–13356.
- 10 R.F.W. Bader; Quantum topology of molecular charge distributions. III. The mechanics of an atom in a molecule. *J. Chem. Phys.* **1980**, 73, 2871–2883.
- 11 P.F. Zou, R.F.W. Bader; Variational principle and path integrals for atoms in molecules. *Int. J. Quantum Chem.* **1992**, 43, 677–699.
- 12 R.F.W. Bader, P.M. Beddall; Virial field relationship for molecular charge distributions and the spatial partitioning of molecular properties. *J. Chem. Phys.* **1972**, 56, 3320–3328.
- 13 R.F.W. Bader, P.M. Beddall, J. Jr. Peslak; Theoretical development of a virial relationship for spatially defined fragments of molecular systems. *J. Chem. Phys.* **1973**, 58, 557–566.
- 14 S. Srebrenik, R.F.W. Bader; Towards the development of the quantum mechanics of a subspace. *J. Chem. Phys.* **1975**, 63, 3945–3961.
- 15 S. Srebrenik, R.F.W. Bader, T.T. Nguyen-Dang; Subspace quantum mechanics and the variational principle. *J. Chem. Phys.* **1978**, 68, 3667–3679.
- 16 R.G. Parr, W. Yang; *Density-Functional Theory of Atoms and Molecules*; Oxford University Press: Oxford, 1989.
- 17 P. Hohenberg, W. Kohn; Inhomogeneous electron gas. *Phys. Rev. B* **1964**, 136, 864–871.
- 18 W. Kohn, L.J. Sham; Self consistent equations including exchange and correlation effects. *Phys. Rev. A* **1965**, 140 (4A), 1133–1138.
- 19 A. Becke; Density-functional thermochemistry.1. The effect of the exchange-only gradient correction. *J. Chem. Phys.* **1992**, 96, 2155–2160.
- 20 A. Becke; Density-functional thermochemistry.2. The effect of the Perdew-Wang generalized-gradient correlation correction. *J. Chem. Phys.* **1992**, 97, 9173–9177.
- 21 A. Becke; A new mixing of Hartree-Fock and local density-functional theories. *J. Chem. Phys.* **1993**, 98, 1372–1377.
- 22 A. Becke; Density-functional thermochemistry.3. The role of exact

- exchange. *J. Chem. Phys.* **1993**, *98*, 5648–5652.
- 23** C. Lee, W. Yang, R. Parr; Development of the Colle–Salvetti correlation-energy formula into a functional of the electron-density. *Phys. Rev. B* **1988**, *37*, 785–789.
- 24** N.K. Hansen, P. Coppens; Testing aspherical atom refinement on small molecules data sets. *Acta Cryst.* **1978**, *A34*, 909–921.
- 25** P. Coppens; *X-ray Charge Densities and Chemical Bonding*; Oxford University Press, Inc.: New York, 1997.
- 26** T.S. Koritsanszky, P. Coppens; Chemical applications of X-ray charge-density analysis. *Chem. Rev.* **2001**, *101*, 1583–1628.
- 27** C. Gatti; Chemical bonding in crystals: New directions. *Z. Kristallogr.* **2005**, *220*, 399–457.
- 28** P. Macchi, A. Angelo Sironi; Chemical bonding in transition metal carbonyl clusters: Complementary analysis of theoretical and experimental electron densities. *Coord. Chem. Rev.* **2003**, *238–239*, 383–412.
- 29** R.F.W. Bader; Can there be more than a single definition of an atom in a molecule? *Can. J. Chem.* **1999**, *77*, 86–93.
- 30** R.J. Gillespie, P.L.A. Popelier; *Molecular Geometry and Chemical Bonding: From Lewis to Electron Densities*; Oxford University Press: New York, 2001.
- 31** R.J. Boyd, R.A. McLelland, N.H. Werstiuk (Guest Editors); *Can. J. Chem.* (Special issue dedicated to Professor Richard F.W. Bader) **1996**, *74*(6).

1

An Introduction to the Quantum Theory of Atoms in Molecules

Chérif F. Matta and Russell J. Boyd

1.1 Introduction

The observation that some properties attributed to atoms and functional groups are transferable from one molecule to another has played a key role in the development of chemistry. This observation provides a basis for group additivity schemes and is exemplified by the constancy of group contributions to thermodynamic and spectroscopic properties. But what is the electronic basis of this empirical transferability? The quantum theory of atoms in molecules (QTAIM) [1], developed by Professor Richard F. W. Bader and his coworkers, relies on quantum observables such as the electron density $\rho(\mathbf{r})$ and energy densities to answer such a question. Other important (related) questions addressed by QTAIM include:

- What is an atom in a molecule or a crystal?
- How can an atom or a group of atoms be transferable sometimes in *very* different external potentials?
- Can one define bonding in molecules unambiguously especially in borderline cases?

This chapter contains a summary of some of the main concepts of QTAIM. A more comprehensive and mathematically elegant treatment can be found in Bader's book [1].

(Often in this chapter, the word "molecule" includes extended systems such as polymers, weakly bonded molecular complexes, and molecular and ionic crystals, in addition to its more traditional meaning of a single, finite, isolated chemically bonded group of atoms. It will be clear from the context when this term is used in its traditional or in its larger sense.)

1.2 The Topology of the Electron Density

The topology of the electron density is dominated by the attractive forces of the nuclei imparting it with its principal topological feature – a substantial local max-

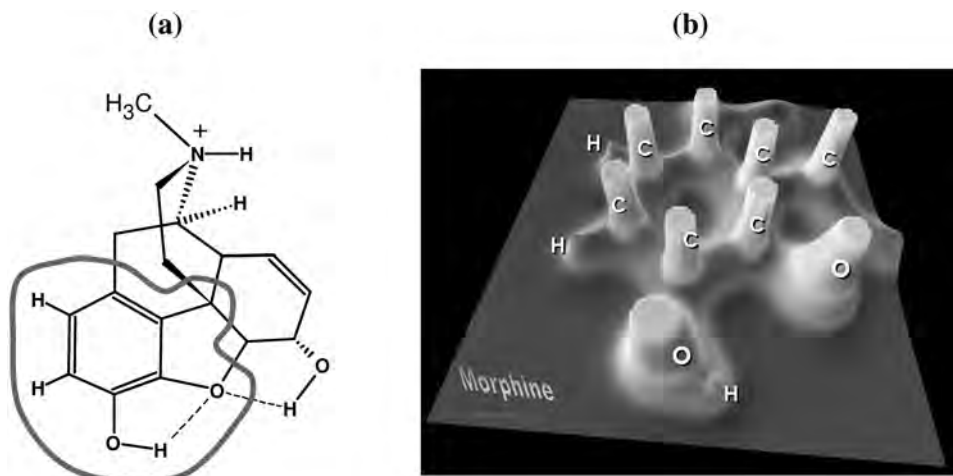


Fig. 1.1 (a) The molecular structure of the morphine molecule with an indication of the region shown in the relief map in (b). (b) A relief map representation of the electron density in the plane of the aromatic ring showing marked maxima at the positions of the carbon and oxygen nuclei (truncated at $\rho(r) = 1.0$ au) and much smaller peaks at the position of the hydrogen nuclei.

imum at the position of each nucleus. A consequence of the dominance of nuclear maxima in the electron density distribution is the association of an atom with a region of space the boundaries of which are determined by the balance in the forces the neighboring nuclei exert on the electrons. Figure 1.1b is a relief map of the electron density of the phenolic region of the morphine molecule, in the plane of the aromatic ring, showing the maxima at the C, O, and H nuclei.

A “critical point” (CP) in the electron density is a point in space at which the first derivatives of the density vanish, i.e.:

$$\nabla\rho = \mathbf{i}\frac{d\rho}{dx} + \mathbf{j}\frac{d\rho}{dy} + \mathbf{k}\frac{d\rho}{dz} \rightarrow \begin{cases} = \vec{0} & \text{(At critical points and} \\ & \text{at } \infty) \\ \text{Generally } \neq \vec{0} & \text{(At all other points)} \end{cases} \quad (1)$$

where the zero vector signifies that each individual derivative in the gradient operator, ∇ , is zero and not just their sum. The gradient of a scalar function such as $\rho(\mathbf{r})$ (Eq. 1) at a point in space is a vector pointing in the direction in which $\rho(\mathbf{r})$ undergoes the greatest rate of increase and having a magnitude equal to the rate of increase in that direction. The maximum at the position of a nucleus constitutes one type of CP, namely, a nuclear critical point (NCP). (The neglect of the finite size of atomic nuclei in quantum chemical calculations, an exceptionally good approximation, results in cusps in the potential and in the electron density $\rho(\mathbf{r})$ at the position of the nuclei. Because of this cusp, the derivatives of the electron

density at the position of a nucleus are not defined and so, in a formal mathematical sense, this position is not a true critical point. The nuclear maxima behave *topologically* as critical points, however.)

One can discriminate between a local minimum, a local maximum, or a saddle point by considering the second derivatives, the elements of the tensor $\nabla\nabla\rho$. There are nine second derivatives of $\rho(\mathbf{r})$ that can be arranged in the so-called ‘‘Hessian matrix’’, which when evaluated at a CP located at \mathbf{r}_c is written:

$$\mathbf{A}(\mathbf{r}_c) = \left(\begin{array}{ccc} \frac{\partial^2\rho}{\partial x^2} & \frac{\partial^2\rho}{\partial x\partial y} & \frac{\partial^2\rho}{\partial x\partial z} \\ \frac{\partial^2\rho}{\partial y\partial x} & \frac{\partial^2\rho}{\partial y^2} & \frac{\partial^2\rho}{\partial y\partial z} \\ \frac{\partial^2\rho}{\partial z\partial x} & \frac{\partial^2\rho}{\partial z\partial y} & \frac{\partial^2\rho}{\partial z^2} \end{array} \right)_{\mathbf{r}=\mathbf{r}_c}. \quad (2)$$

The Hessian matrix can be diagonalized because it is real and symmetric. The diagonalization of $\mathbf{A}(\mathbf{r}_c)$ is equivalent to a rotation of the coordinate system $\mathbf{r}(x, y, z) \rightarrow \mathbf{r}(x', y', z')$ superimposing the new axes x' , y' , z' with the principal curvature axes of the critical point. The rotation of the coordinate system is accomplished via a unitary transformation, $\mathbf{r}' = \mathbf{r}\mathbf{U}$, where \mathbf{U} is a unitary matrix constructed from a set of three eigenvalue equations $\mathbf{A}\mathbf{u}_i = \lambda_i\mathbf{u}_i$ ($i = 1, 2, 3$) in which \mathbf{u}_i is the i th column vector (eigenvector) in \mathbf{U} . A similarity transformation $\mathbf{U}^{-1}\mathbf{A}\mathbf{U} = \mathbf{\Lambda}$ transforms the Hessian into its diagonal form, which is written explicitly as:

$$\mathbf{\Lambda} = \left(\begin{array}{ccc} \frac{\partial^2\rho}{\partial x'^2} & 0 & 0 \\ 0 & \frac{\partial^2\rho}{\partial y'^2} & 0 \\ 0 & 0 & \frac{\partial^2\rho}{\partial z'^2} \end{array} \right)_{\mathbf{r}'=\mathbf{r}_c} = \left(\begin{array}{ccc} \lambda_1 & 0 & 0 \\ 0 & \lambda_2 & 0 \\ 0 & 0 & \lambda_3 \end{array} \right), \quad (3)$$

in which λ_1 , λ_2 , and λ_3 are the curvatures of the density with respect to the three principal axes x' , y' , z' .

An important property of the Hessian is that its trace is invariant to rotations of the coordinate system. The trace of the Hessian of the density is known as the Laplacian of the density $[\nabla^2\rho(\mathbf{r})]$ and, when $x = x'$, $y = y'$, and $z = z'$, is given by:

$$\nabla^2\rho(\mathbf{r}) = \nabla \cdot \nabla\rho(\mathbf{r}) = \underbrace{\frac{\partial^2\rho(\mathbf{r})}{\partial x^2}}_{\lambda_1} + \underbrace{\frac{\partial^2\rho(\mathbf{r})}{\partial y^2}}_{\lambda_2} + \underbrace{\frac{\partial^2\rho(\mathbf{r})}{\partial z^2}}_{\lambda_3} \quad (4)$$

where we have dropped the primes of the principal axes.

Critical points are classified according to their *rank* (ω) and *signature* (σ) and are symbolized by (ω, σ) . The rank is the number of non-zero curvatures of ρ at the critical point. A critical point that has $\omega < 3$ is mathematically unstable and will vanish or bifurcate under small perturbations of the density caused by nuclear motion. The presence of such a CP (with a rank less than three) indicates a change in the topology of the density and, hence, a change in the molecular structure. For this reason, critical points with $\omega < 3$ are generally not found in equilibrium charge distributions and one nearly always finds $\omega = 3$. The signature is the algebraic sum of the signs of the curvatures, i.e. each of the three curvatures contributes ± 1 depending on whether it is a positive or negative curvature.

There are four types of stable critical points having three non-zero eigenvalues:

- $(3, -3)$ Three negative curvatures: ρ is a local maximum.
- $(3, -1)$ Two negative curvatures: ρ is a maximum in the plane defined by the corresponding eigenvectors but is a minimum along the third axis which is perpendicular to this plane.
- $(3, +1)$ Two positive curvatures: ρ is a minimum in the plane defined by the corresponding eigenvectors and a maximum along the third axis which is perpendicular to this plane.
- $(3, +3)$ Three curvatures are positive: ρ is a local minimum.

Each type of critical point described above is identified with an element of chemical structure: $(3, -3)$ *nuclear critical point* (NCP); $(3, -1)$ *bond critical point* (BCP); $(3, +1)$ *ring critical point* (RCP); and $(3, +3)$ *cage critical point* (CCP).

The number and type of critical points that can coexist in a molecule or crystal follow a strict topological relationship which states that:

$$n_{\text{NCP}} - n_{\text{BCP}} + n_{\text{RCP}} - n_{\text{CCP}} = \begin{cases} 1 & \text{(Isolated molecules)} \\ 0 & \text{(Infinite crystals)} \end{cases} \quad (5)$$

where n denotes the number of the subscripted type of CP. The first equality is known as the Poincaré–Hopf relationship (PH) [1] and applies for isolated finite systems such as a molecule, the second equality is known as the Morse equation and applies in cases of infinite periodic lattices [2]. The set $\{n_{\text{NCP}}, n_{\text{BCP}}, n_{\text{RCP}}, n_{\text{CCP}}\}$ for a given system is known as the “characteristic set”.

Violation of Eq. (5) implies an inconsistent characteristic set, that a critical point has been missed, and that a further search for the missing critical point(s) is necessary. On the other hand, the satisfaction of this equation does not *prove* its completeness. For example, if we miss both a BCP and an RCP for a molecule, Eq. (5) becomes $n_{\text{NCP}} - (n_{\text{BCP}} - 1) + (n_{\text{RCP}} - 1) - n_{\text{CCP}} = 1$ which is clearly still valid [3]. The likelihood of missing both a BCP and a RCP is small, however, and, in practice, satisfaction of Eq. (5) is taken as a proof of the consistency *and* completeness of the characteristic set.

A ring critical point will always be found in the interior of a ring of chemically bonded atoms. When several rings are connected in a manner which encloses an

interstitial space, a cage critical point arises in the enclosed space. Figure 1.2 shows the molecular graph (the set of bond paths and critical points) of two molecules: (a) cubane, and (b) 4-methyl-1,12-difluoro[4]helicene. The bond path is a single line of maximum electron density linking the nuclei of two chemically-bonded atoms. (The bond path is discussed in more detail later in this chapter.) In cubane, the bond paths are arranged between the vertices of a cube forming six rings with the consequent appearance of one-ring critical point at the centre of each face of the cube. These six ring surfaces completely enclose the volume of the cube and, as a result, a cage critical point forms in the center of the cube. In Fig. 1.2a, the reader may also note the marked curvature of the bond paths in cubane, indicative of a significant ring strain in this unstable molecule.

All cage critical points reported in the literature until 2005 were found to be enclosed by at least three ring surfaces, as stated by Bader in 1990 [1]: “*While it is mathematically possible for a cage to be bounded by only two ring surfaces, the minimum number found in an actual molecule so far is three, as in bicyclo [1.1.1] pentane, for example*”, a statement reiterated in 2000 [3]. In Fig. 1.2b there is nothing unusual about the aromatic system, but the nuclei of the two fluorine atoms in the “Fjord region” are linked by a bond path [4] closing a seven-membered ring which has quite an unusual topology – it gives rise to *two ring* critical points and *a cage* critical point [5]. We have, thus, recently reported the first example of an actual molecular system in which a cage is bounded by only *two* ring surfaces [5]. Such a CCP (enclosed by two ring surfaces) arises in all the studied derivatives of 1,12-difluoro[4]helicenes [5]. In these molecules, the seven-membered ring in the Fjord region is so distorted out of planarity that its ring surface splits into two, giving rise to this CCP [5]. In all cases, the Poincaré–Hopf relationship is satisfied [5].

1.3

The Topology of the Electron Density Dictates the Form of Atoms in Molecules

The pronounced maxima in the electron density at the positions of the nuclei give rise to a rich topology. This topology embodies a natural partitioning of the molecular space into separate mononuclear regions, Ω , identified as atoms in molecules. The surface bounding an atom in a molecule is one of zero flux in the gradient vector field of the electron density, i.e. it is not crossed by any of the gradient vectors $[\nabla\rho(\mathbf{r})]$ at any point, a statement which is equivalent to satisfying the condition:

$$\nabla\rho(\mathbf{r}) \cdot \mathbf{n}(\mathbf{r}) = 0, \quad \text{for all } \mathbf{r} \text{ belonging to the surface } S(\Omega) \quad (6)$$

where \mathbf{r} is the position vector and $\mathbf{n}(\mathbf{r})$ the unit vector normal to the surface $S(\Omega)$.

The plot in Fig. 1.3a represents the electron density and its gradient vector field in the molecular plane of BF_3 . The figure contrasts the zero-flux surfaces which partition the molecular space into separate mononuclear “atomic basins” and an arbitrary surface cutting through the density. The left side of Fig. 1.3a is a contour

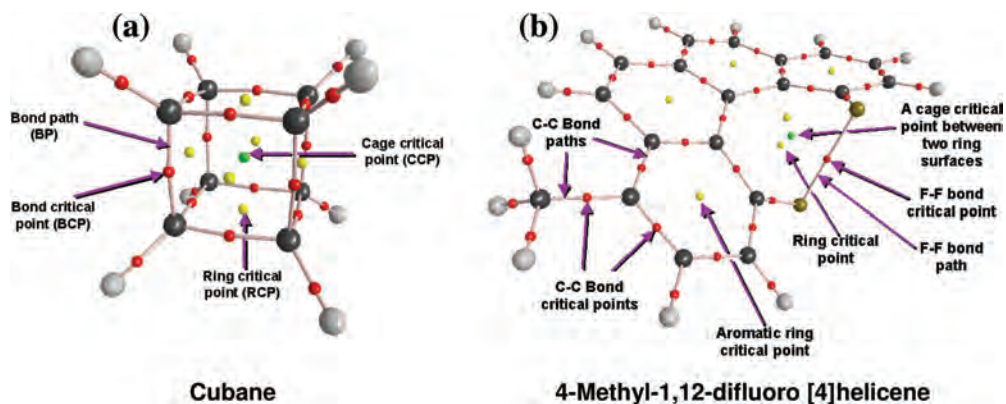


Fig. 1.2 The molecular graph of (a) cubane and (b) 4-methyl-1,12-difluoro[4]helicene showing the bond paths (lines) and the different critical points: nuclear (color-coded by element: C = black, H = grey, F = golden), bond (small red dots), ring (yellow dots), and cage (green dots) critical points.

plot of $\rho(\mathbf{r})$, the contours decreasing in value from the nuclei outward. Instead of plotting $\rho(\mathbf{r})$ in the right half of Fig. 1.3a (which is a mirror image of the left side by virtue of the molecular symmetry), we have depicted, instead, the corresponding gradient vector field $\nabla\rho(\mathbf{r})$. The gradient vector field lines partition the molecular space naturally into three fluorine basins and a central boron basin (Fig. 1.3a).

Gradient vector field lines belonging to an atomic basin all converge to *one* nucleus which acts as an attractor to these gradient vector field lines. In doing so, these gradient vector field lines sweep a portion of physical space associated with one nucleus and which is identified as the basin of an atom in a molecule (AIM). Three-dimensional volume renderings of the atoms and groups of atoms within the BF_3 molecule are shown in Fig. 1.3b. An atom in a molecule is defined as the union of a nucleus and its associated basin. Each basin is bounded by one (or by the union of a number of) zero-flux surface(s) one of which may occur at infinity. An atom in a molecule may be defined, alternatively and equivalently, as a region of space bounded by one or more zero-flux surface(s).

Occasionally, local maxima in the electron density can occur at positions other than those of atomic nuclei, especially in metals [6, 7] and semiconductors [8, 9], but also in systems such as the solvated electron [10] and at the positions of defects in crystals and color F-centers [11]. The non-nuclear maxima, also known as non-nuclear attractors (NNA), are topologically indistinguishable from the nuclear maxima. Just like a nucleus, an NNA is associated with a basin swept by gradient vector field lines and is bounded by a zero-flux surface. Consequently, NNA

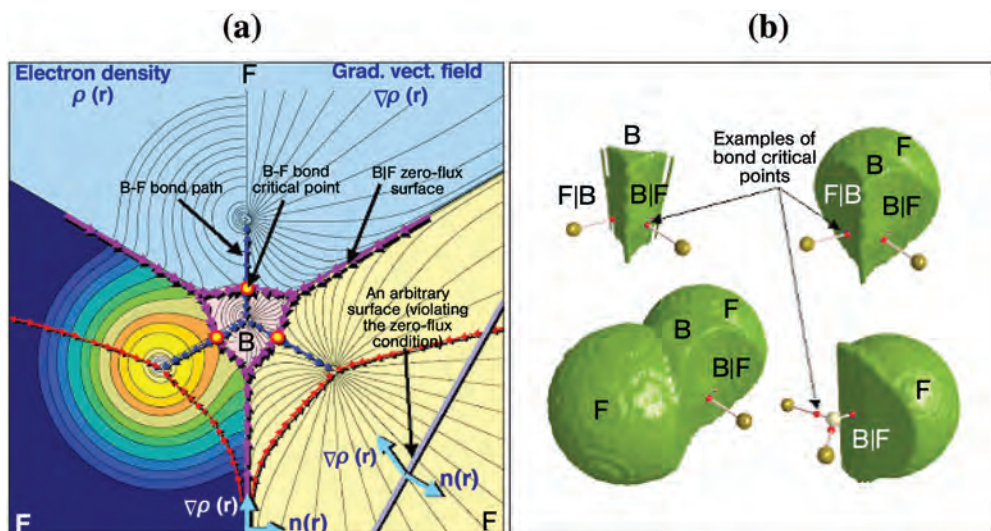


Fig. 1.3 (a) The electron density (left) and the gradient vector field (right) of the density in the molecular plane of BF_3 . The blue arrows connecting the nuclei trace the bond paths. The magenta arrows delimiting atomic basins trace the intersections of the zero-flux surfaces with the plane. The contours increase from the outermost 0.001 au contour followed by 2×10^n , 4×10^n , and 8×10^n au with n starting at -3 and increasing in steps of unity. The small circles drawn on the three bond paths are the B–F bond critical points (BCP). The intersection of an arbitrary surface with the plane of the figure, the straight line on the lower right part

of (a), is shown to be crossed by gradient vectors and is contrasted with a zero-flux surface. (b) Four three-dimensional renderings of the density of atoms and groupings of atoms in BF_3 . The outer surface is the 0.002 au isodensity envelope. The zero-flux surfaces are denoted by the vertical bars between the atomic symbols. Large spheres represent the nuclei of the fluorine atoms (golden) and of the boron atom (blue-gray). The lines linking the nuclei represent the bond paths. The BCPs are denoted by the small red dots. A BCP always lies on the zero-flux surface shared by the two bonded atoms.

basins constitute proper open quantum systems and are therefore termed “pseudo-atoms”. Pseudo-atoms can be bonded (i.e. share a common interatomic zero-flux surface, a bond critical point, and a bond path) to atoms and other pseudo-atoms in a molecule. Non-nuclear attractors and their basins are of great importance in characterizing metallic bonding and are of substantial theoretical interest. A detailed discussion of NNA can be found in Chapter 7 of this book.

There is a unique set of gradient vectors lines which originate at infinity and terminate at a point *between* two bonded atoms, the lines of this set fall by definition on the zero-flux surface because they satisfy Eq. (6) locally. It should be noted that the three zero-flux surfaces depicted in Fig. 1.3 are between the boron and fluorine atoms, the boron atom being bounded three zero-flux surfaces which merge in pairs at infinity between fluorine basins. There are no zero-flux surfaces

between any pair of fluorine atoms in BF_3 , these surfaces only exist between bonded atoms and are characteristic of bonding interactions.

The topological definition of an atom follows from the boundary condition expressed in Eq. (6) and which applies to every point on the surface. This real space partitioning of the electron density has been shown to be rooted in quantum mechanics bringing into coincidence the topological definition of an atom in a molecule with that of a proper open quantum system (see Chapter 2 and also the detailed derivation of the quantum mechanics of proper open systems [12] from Schwinger's principle of stationary action [13]).

1.4

The Bond and Virial Paths, and the Molecular and Virial Graphs

The presence of an interatomic zero-flux surface between any two bonded atoms in a molecule is always accompanied by another key topological feature – there is, *in real space*, a single line of *locally* maximum density, termed the “bond path” (BP), linking their nuclei. The bond path is a universal indicator of chemical bonding of all kinds; weak, strong, closed-shell, and open-shell interactions [14]. The point on the bond path with the lowest value of the electron density (minimum along the path) is the bond critical point (BCP) and it is at that point where the bond path intersects the zero-flux surface separating the two bonded atoms.

The collection of bond paths linking the nuclei of bonded atoms in an equilibrium geometry, with the associated critical points, is known as the *molecular graph*. (In a non-equilibrium geometry, lines of maximum electron density linking the nuclei are known as “atomic interaction lines”, because these may or may not persist when the geometry is energy-minimized, i.e. optimized.) The molecular graph provides an unambiguous definition of the “molecular structure” and can thus be used to locate changes in structure along a reaction path.

Mirroring every molecular graph is a “shadow” graph, again in real space, but this time the graph is defined by a set of lines of maximally negative *potential energy density*. In other words, there is a single line of maximally negative potential energy density linking the same attractors which share a bond path [15]. This line of “maximum stability” in real space is termed a “*virial path*”. The collection of virial paths and the associated critical points constitute the *virial graph*. The virial graph defines the same molecular structure as the molecular graph, the virial field and the electron density being homeomorphic [15].

Figure 1.4 shows the chemical structure and the molecular and virial graphs of the phenanthrene molecule. This polycyclic aromatic hydrocarbon molecule has a bond path between the two hydrogen atoms in the bay region, a mode of closed-shell bonding which has been recently characterized in detail and termed hydrogen–hydrogen bonding (to be contrasted with dihydrogen bonding) [16, 17]. The virial graph is shown to faithfully map each bond path with a corresponding virial path including the bond path of a weak closed-shell bonding interaction such as the hydrogen–hydrogen bonding interaction (Fig. 1.4).

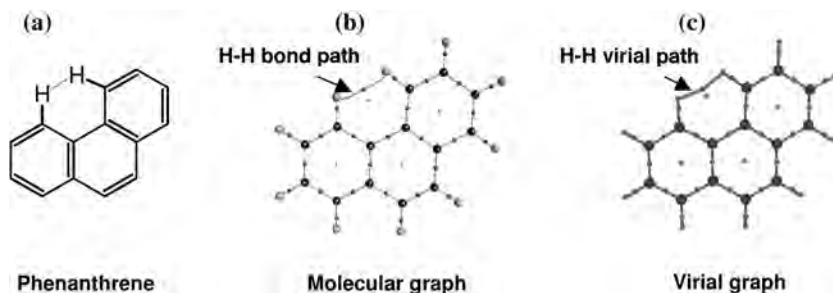


Fig. 1.4 (a) The chemical structure of phenanthrene. (b) The molecular graph of phenanthrene showing the collection of bond paths and associated critical points. (c) The corresponding virial graph.

We conclude this section by stating that *atoms that are chemically bonded have their nuclei linked by a (single) bond path and by an accompanying virial path and they share a bond critical point and a common interatomic zero-flux surface.*

1.5

The Atomic Partitioning of Molecular Properties

The quantum theory of atoms in molecules is a generalization of quantum mechanics to open quantum systems. Bader has shown that the topological partitioning of the molecules into atomic basins is essential for development of the quantum mechanics of open systems [12]. The zero-flux condition, Eq. (6), is the necessary constraint for the application of Schwinger's principle of stationary action [13] to part of a quantum system [12].

The partitioning of the molecular space into atomic basins enables the partitioning of electronic properties into atomic contributions in one consistent theoretical framework. Among the properties often discussed are the atomic charges and higher multipolar electric polarizations, atomic volumes, atomic total energies (and the different contributions to the atomic energies), and the electron localization within one basin or delocalization between two basins [1, 18].

The expectation value of an operator averaged over all space is given by the sum of the expectation values of this operator averaged over all the atoms in the molecule or the crystal, in atomic units:

$$\langle \hat{O} \rangle_{molecule} = \sum_i^{\text{all atoms in the molecule}} \left(N \int_{\Omega_i} \left\{ \int \frac{1}{2} [\Psi^* \hat{O} \Psi + (\hat{O} \Psi)^* \Psi] d\tau' \right\} d\mathbf{r} \right) \quad (7a)$$

$$= \sum_i^{\text{all atoms in the molecule}} \left(\int_{\Omega_i} \rho_O d\mathbf{x} \right) = \sum_i^{\text{all atoms in the molecule}} O(\Omega_i) \quad (7b)$$

where $\langle \hat{O} \rangle_{\text{molecule}}$ is the molecular expectation value of the operator \hat{O} , $O(\Omega_i)$ is the average of this operator over an atom Ω_i , and where the sum runs over all the atoms in the molecule or crystal. Integration over the coordinates of all electrons but one and summation over all spins is symbolized by $\int d\tau'$. Equation (7b) implies that any molecular property O which can be expressed in terms of a corresponding property density in space $\rho_O(\mathbf{r})$ can be written as a sum of atomic contributions obtained by averaging the appropriate operator over the volume of the atom, i.e. it exhibits atomic additivity.

1.6

The Nodal Surface in the Laplacian as the Reactive Surface of a Molecule

Because the Laplacian is essentially a second derivative, its sign indicates regions of local electronic charge concentration or depletion with respect to the immediate neighborhood. Thus, where $\nabla^2\rho(\mathbf{r}) > 0$ the density is locally depleted and expanded relative to its average distribution; where $\nabla^2\rho(\mathbf{r}) < 0$ the density is locally concentrated, tightly bound, and compressed relative to its average distribution. A local charge concentration behaves as a Lewis base (electron donor) whereas a local charge depletion acts as a Lewis acid (electron acceptor).

The Laplacian reproduces the spherical shell structure of isolated atoms in terms of alternating shells of charge concentration followed by shells of charge depletion [19, 20]. The spherical nodes in the Laplacian are envelopes bounding regions of density depletion or concentration. The outer shell of charge concentration, which is followed by a shell of charge depletion extending to infinity, is called the valence shell charge concentration (VSCC). When an atom is involved in bonding the spherical symmetry of the VSCC is broken. A chemical reaction corresponds to the combination of a “lump” in the VSCC of the base with a “hole” in the VSCC of the acid.

Covalently bonded atoms have bonding charge concentrated in the region between their nuclei. In addition to bonding charge concentrations, lone pairs are associated with non-bonding charge concentrations. These observations reflect an underlying mapping between the Laplacian of the electron density and the Laplacian of the conditional pair density when electrons tend to be localized [21].

The Laplacian of the density is characterized by a rich topology which provides a basis for the VSEPR model [22–24] of molecular geometry [1, 25–27]. More details on this topic are available elsewhere [1, 3, 25–29] and Chapter 19 explores the use of the reactive surface in drug design and drug–receptor molecular complementarity.

1.7

Bond Properties

A zero-flux surface is defined by a particular set of $\nabla\rho(\mathbf{r})$ trajectories all the members of which terminate at a single point, the bond critical point, where

$\nabla\rho(\mathbf{r}) = 0$. There is one BCP between each pair of atoms that are bonded, i.e., two atoms linked by a bond path and sharing a common interatomic zero-flux surface. In addition to the set of trajectories which terminate at the BCP and define an interatomic surface, a pair of trajectories originates at the BCP with each member of the pair terminating at one of the nuclei of the chemically bonded atoms. This latter pair of trajectories defines the bond path [14]. Chemical bonding interactions are characterized and classified according to the properties of the electron and energy densities at the BCP, collectively known as “bond properties”.

1.7.1

The Electron Density at the BCP (ρ_b)

The strength of a chemical bond, its bond order (BO), is reflected in the electron density at the BCP (ρ_b) [1]:

$$\text{BO} = \exp[A(\rho_b - B)] \quad (8)$$

where A and B are constants which depend on the nature of the bonded atoms. In general, ρ_b is greater than 0.20 au in shared (covalent) bonding and less than 0.10 au in a closed-shell interaction (for example ionic, van der Waals, hydrogen, dihydrogen, H–H bonding, etc.). ρ_b has been shown to be strongly correlated with the binding energy for several types of bonding interaction [30–36] and with the bond length of S–S bonding interactions [37]. Proposals to generalize Eq. (8) by including more than two elements in the same fitting have recently appeared in the literature [38, 39].

1.7.2

The Bonded Radius of an Atom (r_b), and the Bond Path Length

The distance of a BCP from nucleus A determines the “bonded radius” of atom A relative to the interaction defined by the BCP, and is denoted $r_b(\text{A})$. If the bond path is coincident with the internuclear axis, then the sum of the two associated bond radii, termed the bond path length, equals the bond length. If, however, the bond path is curved, or strained chemically, the bond path length will exceed the bond length. Examples of this latter behavior are found for hydrogen-bonded interactions and for bonding within strained cyclic molecules (e.g. the curved C–C bond paths in the cubane molecule, Fig. 1.2a).

1.7.3

The Laplacian of the Electron Density at the BCP ($\nabla^2\rho_b$)

The Laplacian at the BCP is the sum of the three curvatures of the density at the critical point (Eq. 4), the two perpendicular to the bond path, λ_1 and λ_2 , being negative (by convention, $|\lambda_1| > |\lambda_2|$) whereas the third, λ_3 , lying along the bond

path, is positive. The negative curvatures measure the extent to which the density is concentrated along the bond path and the positive curvature measures the extent to which it is depleted in the region of the interatomic surface and concentrated in the individual atomic basins.

In covalent bonding the two negative curvatures are dominant and $\nabla^2\rho_b < 0$, for example, $\nabla^2\rho_b = -1.1$ au for a typical C–H bond. In contrast, in closed-shell bonding, for example ionic, hydrogen-bonding or van der Waals interactions, the interaction is characterized by a depletion of density in the region of contact of the two atoms and $\nabla^2\rho_b > 0$. An N–(H \cdots O)=C hydrogen bond, for instance, is characterized by $\nabla^2\rho_b = +0.03$ au. In strongly polar bonding, (e.g. C–X, where X = O, N, F), there is a significant accumulation of electron density between the nuclei, as in all shared interactions, but the Laplacian in this type of bonding can be of either sign.

1.7.4

The Bond Ellipticity (ε)

The ellipticity measures the extent to which density is preferentially accumulated in a given plane containing the bond path. The ellipticity is defined as:

$$\varepsilon = \frac{\lambda_1}{\lambda_2} - 1 \quad (\text{where } |\lambda_1| \geq |\lambda_2|) \quad (9)$$

If $\lambda_1 = \lambda_2$, then $\varepsilon = 0$, and the bond is cylindrically symmetrical; examples are the C–C single bond in ethane or the triple bond in acetylene. Thus, ε is a measure of the π -character of the bonding up to the limit of the “double bond” for which the ellipticity reaches a maximum. On going from a double to a triple bond, the trend is reversed and the ellipticity decreases with increasing bond order, because at the limit of BO = 3 the bonding regains its cylindrical symmetry (two π -bonding interactions in two orthogonal planes in addition to a cylindrically symmetric σ -bonding interaction). The ellipticity of an aromatic bond is ca. 0.23 in benzene and that of a formal double bond is ca. 0.45 in ethylene.

1.7.5

Energy Densities at the BCP

Energy densities require information contained in the one-electron density matrix (and not just the density, its diagonal elements). The energy densities (potential, kinetic, and total) are used to summarize the mechanics of a bonding interaction.

The potential energy density, $\mathcal{V}(\mathbf{r})$, also known as the virial field, is the average effective potential field experienced by a single electron at point \mathbf{r} in a many-particle system. The virial field evaluated at any point in space is always negative and its integral over all space yields the total potential energy of the molecule. The local statement of the virial theorem expresses the relationship between the

virial field, the kinetic energy density, and the Laplacian, which when written for a stationary state is [1, 12, 40]:

$$\left(\frac{\hbar^2}{4m}\right)\nabla^2\rho(\mathbf{r}) = 2G(\mathbf{r}) + \mathcal{V}(\mathbf{r}) \quad (10)$$

where

$$G(\mathbf{r}) = \frac{\hbar^2}{2m} N \int d\tau' \nabla\Psi^* \cdot \nabla\Psi \quad (11)$$

and where $G(\mathbf{r})$ is the gradient kinetic energy density and Ψ is an antisymmetric many-electron wavefunction.

Because we always have $G(\mathbf{r}) > 0$ and $\mathcal{V}(\mathbf{r}) < 0$, the local virial theorem when applied at a BCP implies that interactions for which $\nabla^2\rho_b < 0$ are dominated by a local reduction of the potential energy. Conversely, interactions for which $\nabla^2\rho_b > 0$ are dominated by a local excess in the kinetic energy.

To compare the kinetic and potential energy densities on an equal footing (instead of the 2:1 virial ratio) Cremer and Kraka [41] proposed evaluating the total electronic energy density [$H(\mathbf{r}) = G(\mathbf{r}) + \mathcal{V}(\mathbf{r})$] at the BCP:

$$H_b = G_b + \mathcal{V}_b \quad (12)$$

The total energy density yields the total electronic energy when integrated over all space. H_b is negative for interactions with significant sharing of electrons, its magnitude reflecting the “covalence” of the interaction [41].

1.7.6

Electron Delocalization between Bonded Atoms: A Direct Measure of Bond Order

The number of electron pairs *shared* between two bonded atoms is often called the *bond order*. QTAIM provides a bookkeeping of the number of pairs shared between two atoms by integrating the exchange density once over each of the two atomic basins. This property may as well be classified under “atomic properties” because it involves the double integration of the exchange density over the basins of two atoms, but, because it “counts” the number of electron pairs shared between two atoms, when reported for *bonded* atoms, it can be regarded as a bond property.

The magnitude of the exchange of the electrons in the basin of atom A with those in the basin of atom B is termed the delocalization index between them, $\delta(A, B)$, and is defined for a closed-shell system as [42]:

$$\delta(A, B) = 2|F^\alpha(A, B)| + 2|F^\beta(A, B)| \quad (13)$$

where the Fermi correlation is defined as:

$$\begin{aligned} F^\sigma(A, B) &= - \sum_i \sum_j \int_A d\mathbf{r}_1 \int_B d\mathbf{r}_2 \{ \phi_i^*(\mathbf{r}_1) \phi_j(\mathbf{r}_1) \phi_j^*(\mathbf{r}_2) \phi_i(\mathbf{r}_2) \} \\ &= - \sum_i \sum_j S_{ij}(A) S_{ji}(B) \end{aligned} \quad (14)$$

where $S_{ij}(\Omega) = S_{ji}(\Omega)$ is the overlap integral of two spin orbitals over a region Ω and σ represents spin (α or β).

The second-order density matrix obtained from a configuration interaction (CI) calculation can also be expressed in terms of products of basis functions multiplied by the appropriate coefficients enabling one to express the integrated pair density in terms of overlap contributions. Thus, terms similar to those in Eq. (14) multiplied by the appropriate coefficients appear in the CI expression for $F^\sigma(A, B)$ and electron delocalization is still described in terms of the exchange of electrons between molecular orbitals, but this time in a wavefunction incorporating Coulomb in addition to Fermi correlation [42].

If the double integration in Eq. (14) is performed over only one atomic basin, say atom A , this would yield the total Fermi correlation for the electrons in region A [43]:

$$F^\sigma(A, A) = \int_A d\mathbf{r}_1 \int_A d\mathbf{r}_2 \rho^\sigma(\mathbf{r}_1) h^\sigma(\mathbf{r}_1, \mathbf{r}_2) \quad (15)$$

where its limiting value is $-N^\sigma(A)$, the negative of the σ -spin population of atom A , i.e. the number of σ electrons in A being totally localized within this atom because all remaining σ -spin density would then be excluded from A . In other words, if this limiting value is reached, it implies that the electrons in A do not exchange with electrons outside A . Thus a *localization index* [$\lambda(A)$] is defined as:

$$\lambda(A, A) = |F^\alpha(A, A)| + |F^\beta(A, A)| \quad (16)$$

The limit of total localization, while approached quite closely ($\geq 95\%$) in ionic systems, cannot usually be achieved and one finds that $|F^\sigma(A, A)| < N^\sigma(A)$, indicating that the electrons in region A always exchange, to some extent, with electrons outside the boundaries of A , i.e., they are delocalized.

Because the Fermi correlation counts all electrons, the sum of the localization indices and half of all the delocalization indices is N , the total number of electrons in the molecule. This, in turn, provides a measure of how these electrons are localized within the individual atomic basins and delocalized between them, in effect resulting in bookkeeping of electrons in the molecule:

$$N(A) = \lambda(A) + \frac{1}{2} \sum_{B \neq A} \delta(A, B) \quad (17)$$

How closely the sum of the localization and the delocalization indices (Eq. 17) recovers the total molecular electron population is a global measure of the quality of the atomic integrations.

The localization and delocalization indices can be calculated from the atomic overlap matrices using readily available software such as AIMDELOC [44] or LIDICALC [45, 46].

It is important to realize that a delocalization index can be calculated between *any* pair of atoms whether bonded or not. When $\delta(A, B)$ is calculated between *bonded* atoms it yields a measure of the bond order between them if the electron pairs are equally shared (i.e. there is no appreciable charge transfer) [42, 47].

Because ρ_b and the bond order are strongly correlated (Eq. 8), Matta and Hernández-Trujillo [48] suggested calibrating this correlation using the delocalization index rather than arbitrarily assigned bond orders:

$$\delta(A, B) = \exp[A(\rho_b - B)] \quad (18)$$

Equation (18) enables calibration of experimental ρ_b with delocalization indices obtained by calculation. The fitted equation can then be used to obtain experimental estimates for information on electron sharing contained in a full density matrix, information which is not accessible in a conventional X-ray diffraction experiment, from experimentally determined ρ_b [48]. Data for the 21 carbon-carbon bonds in the estrone hormone could be fitted to the following equation [49]:

$$\delta(C, C') = \exp\{4.7427 \times [\rho_b(\text{in a.u.}) - 0.2538]\} \quad (19)$$

with $r^2 = 0.939$, a variance of 0.002, and a root mean square deviation of 0.010, and in which $\delta(C, C')$ were calculated at the B3LYP/6-311++G(*d, p*) level and ρ_b are the experimentally determined electron density values at the C-C BCPs.

1.8 Atomic Properties

The average of a property O over an atomic basin Ω , $O(\Omega)$, is calculated from:

$$O(\Omega) = \langle \hat{O} \rangle_{\Omega} = \frac{N}{2} \int_{\Omega} d\mathbf{r} \int d\mathbf{r}' [\Psi^* \hat{O} \Psi + (\hat{O} \Psi)^* \Psi] \quad (20)$$

where \hat{O} is a one-electron operator or a sum of one-electron operators. Some examples of commonly computed atomic properties are discussed in the subsections below.

1.8.1

Atomic Electron Population [$N(\Omega)$] and Charge [$q(\Omega)$]

The total electron population of an atom in a molecule is obtained by setting $\hat{O} = \hat{1}$ in Eq. (20). This yields:

$$N(\Omega) = \int_{\Omega} \rho(\mathbf{r}) d\mathbf{r} \quad (21)$$

which can also be expressed explicitly in terms of the separate spin populations as the expectation value of the number operator, an integral operator, averaged over a proper open quantum subsystem:

$$N(\Omega) = \sum_i [\langle \psi_i(\mathbf{r}) | \psi_i(\mathbf{r}) \rangle_{\Omega}^{\alpha} + \langle \psi_i(\mathbf{r}) | \psi_i(\mathbf{r}) \rangle_{\Omega}^{\beta}] \quad (22)$$

in which the separate spin populations are given by:

$$\langle \psi_i(\mathbf{r}) | \psi_i(\mathbf{r}) \rangle_{\Omega}^{\sigma} = \int_{\Omega} \psi_i^{\sigma*}(\mathbf{r}) \psi_i^{\sigma}(\mathbf{r}) d\mathbf{r} \equiv S_{ii}^{\sigma}(\Omega) \quad (23)$$

where σ refers to either α -spin or β -spin, and $S_{ii}^{\sigma}(\Omega)$ is the i th diagonal element of the atomic overlap matrix.

The atomic charge is obtained by subtracting $N(\Omega)$ from the nuclear charge Z_{Ω} :

$$q(\Omega) = Z_{\Omega} - N(\Omega) \quad (24)$$

Because of the manner by which atomic populations are defined, Eqs (22) and (23), QTAIM populations and charges are true quantum expectation values. That is, they are “observables” in the quantum mechanical sense [18, 50]. Observables are not necessarily measurable in practice, but any measurable quantity is an observable or can be expressed in terms of one or more observables. Indirect experimental evidence lends strong support to the physical nature of QTAIM atomic populations and charges [51] (see also Section 1.9.2).

The deviation of the sum of the atomic populations (or charges) from the corresponding molecular value is an indicator of the quality of the numerical integrations. Deviations of less than ca. 0.001–0.002 electrons are regarded as acceptable for molecules of medium size (up to ~ 100 first to third row atoms).

1.8.2

Atomic Volume [Vol. (Ω)]

The atomic volume is defined as the space bounded by the intersection of the zero-flux surface(s) bounding the atom from the molecular interior and a chosen

outer isodensity envelope (if a side of this atom's basin extends to infinity). While a molecule extends in principle to infinity, an outer isodensity of $\rho(\mathbf{r}) = 0.001$ au is usually chosen as its outer bounding surface for two reasons:

1. this isosurface closely recovers the experimental van der Waals volumes in the gas phase, and
2. it usually encloses more than 99% of the electron population of the molecule [1].

The van der Waals surface in condensed phases is closer to the 0.002 au isodensity envelope [1].

1.8.3

Kinetic Energy [$T(\Omega)$]

There are at least two forms of the kinetic energy operator [52] with two corresponding expressions for the atomic average of the kinetic energy, the Schrödinger kinetic energy:

$$K(\Omega) = -\frac{\hbar^2}{4m} N \int_{\Omega} d\mathbf{r} \int d\tau' [\Psi \nabla^2 \Psi^* + \Psi^* \nabla^2 \Psi] \quad (25)$$

and the gradient kinetic energy:

$$G(\Omega) = \frac{\hbar^2}{2m} N \int_{\Omega} d\mathbf{r} \int d\tau' \nabla_i \Psi^* \cdot \nabla_i \Psi \quad (26)$$

For the total system and for a proper open quantum system, Eqs (25) and (26) must yield an identical value for the kinetic energy, of course, i.e. $K(\Omega) = G(\Omega) = T(\Omega)$. Because the difference between $K(\Omega)$ and $G(\Omega)$ should vanish for an atom in a molecule, the (small) departure from zero of this difference as gauged by the Laplacian (Section 1.8.4) is a measure of the numerical accuracy of the atomic integrations.

1.8.4

Laplacian [$L(\Omega)$]

The Laplacian function has the dimensions of electrons \times (length)⁻⁵. Because of the zero-flux boundary condition, Eq. (6), the Laplacian of the electron density, vanishes when integrated over an atomic basin, as can be seen from:

$$\begin{aligned} L(\Omega) &= K(\Omega) - G(\Omega) \\ &= -\frac{\hbar^2}{4m} \int_{\Omega} d\mathbf{r} [\nabla^2 \rho(\mathbf{r})] \\ &= -\frac{\hbar^2}{4m} \int dS(\Omega, \mathbf{r}) \nabla \rho(\mathbf{r}) \cdot \mathbf{n}(\mathbf{r}) = 0 \end{aligned} \quad (27)$$

the last equality is valid only for the total system or if the integration is performed over a proper open quantum system bounded by zero-flux surfaces.

How close the integrated Laplacian approaches zero is often used as an indicator of the numerical accuracy of atomic integrations. Deviations from zero are a measure of integration error. $L(\Omega) \leq \text{ca. } 1.0 \times 10^{-3}$ au for second and third-row atoms and $L(\Omega) \leq \text{ca. } 1.0 \times 10^{-4}$ au for hydrogen atoms are regarded as acceptable and are usually paralleled by atomic energies which add up to within a kcal mol⁻¹ of the directly calculated molecular total energy for a medium size molecule (~100 atoms or fewer). The smaller $L(\Omega)$ the better the quality of an atomic integration.

1.8.5

Total Atomic Energy [$E_e(\Omega)$]

The partitioning of the total molecular energy into a set of additive atomic energies is a non-trivial problem that was solved by Bader [1]. To see the difficulties in partitioning the total energy, one may ask, for instance, how can the nuclear-nuclear repulsion contribution to the total molecular energy be partitioned on an atom-by-atom basis?

The kinetic energy density can be expressed:

$$K(\mathbf{r}) = -\frac{\hbar^2}{4m} N \int d\tau' [\Psi \nabla^2 \Psi^* + \Psi^* \nabla^2 \Psi] \quad (28)$$

which when compared with Eq. (11) yields:

$$K(\mathbf{r}) = G(\mathbf{r}) - \frac{\hbar^2}{4m} \nabla^2 \rho(\mathbf{r}) \quad (29)$$

It is clear from Eq. (29) that the integral of the kinetic energy densities $K(\mathbf{r})$ and $G(\mathbf{r})$ over a volume ω would usually yield different values because the integral of the Laplacian does not usually vanish when integrated over an arbitrary volume, in which case the kinetic energy is *not* well defined. The kinetic energy is well defined if, and only if, the integral of the Laplacian term vanishes, i.e. when this integral is performed over the total system or over an atomic basin bounded by a zero-flux surface. Integrating Eq. (29) over ω , one obtains:

$$K(\omega) = G(\omega) - \frac{\hbar^2}{4m} N \int_{\omega} d\mathbf{r} \nabla \cdot \nabla \rho \quad (30)$$

Using Gauss's theorem, the volume integral in Eq. (30) can be transformed into a surface integral:

$$K(\omega) = G(\omega) - \frac{\hbar^2}{4m} N \int dS(\omega, \mathbf{r}) \nabla \rho \cdot \mathbf{n}(\mathbf{r}) \quad (31)$$

Now it is clear that the second term in the R.H.S. will vanish only for systems bounded by a zero-flux surface satisfying Eq. (6) (or for the whole system, because the Laplacian integrated over the entire space also vanishes). Thus only the total system and proper open sub-systems will have a definite kinetic energy. A proper open system (one bounded by a zero-flux surface and/or infinity) will be referred to as Ω to distinguish it from an arbitrary bounded region of space ω . For such a proper open system one has:

$$K(\Omega) = G(\Omega) = T(\Omega) \quad (32)$$

and, because the integral of the Laplacian vanishes over Ω , the integral of the local statement of the virial theorem (Eq. 10) over Ω yields the *atomic virial theorem*:

$$-2T(\Omega) = \mathcal{V}(\Omega) \quad (33)$$

where the $\mathcal{V}(\Omega)$ is the total atomic virial.

The atomic electronic energy $E_e(\Omega)$ is given by:

$$E_e(\Omega) = T(\Omega) + \mathcal{V}(\Omega) \quad (34)$$

For systems in equilibrium there are no Hellmann–Feynman forces acting on the nuclei and the virial equals the average potential energy of the molecule, i.e. $\mathcal{V} = V$. Under this condition Eq. (33) becomes:

$$-2T(\Omega) = V(\Omega) \quad (35)$$

where $V(\Omega)$ is the potential energy of atom Ω , and Eq. (34) becomes:

$$E(\Omega) = E_e(\Omega) = T(\Omega) + V(\Omega) = -T(\Omega) = \frac{1}{2}V(\Omega) \quad (36)$$

where $E(\Omega)$ is the total energy of atom Ω .

Thus, the energy of an atom in a molecule at its equilibrium geometry is obtained from the atomic statement of the virial theorem, and $E(\Omega) = -T(\Omega)$. The sum of atomic energies yields, naturally, the total energy of the molecule (obtained directly from the electronic structure calculation) to within a small numerical integration error. This additivity of the atomic energies is expressed as:

$$E_{total} = \sum_{\Omega} E(\Omega) \quad (37)$$

The result shown in Eq. (37) is remarkable. The equation expresses the partitioning of the total molecular energy into atomic contributions, a partitioning which includes, for example, the nuclear–nuclear repulsion contribution to the

molecular energy. Such partitioning of the total energy is indispensable if one is to understand the atomic origins of the energy difference between two isomers [4, 16, 53], for example, or the atomic origins of potential energy barriers [17, 54].

The deviation of the sum of the atomic energies from the directly calculated total molecular energy is another global measure of the quality of atomic integrations. A deviation of no more than ca. 1 kcal mol⁻¹ is usually regarded as an indicator of accurate integrations.

The discussion above is based upon the assumption that the calculated molecular wavefunction satisfies the virial theorem exactly, i.e. the molecular virial ratio $-V/T = 2$ to infinite accuracy. In practice, the calculated virial ratio deviates slightly from this ideal value of 2 because of the truncation of the basis set, residual forces on the nuclei, and the finite nature of the convergence thresholds in a typical calculation. The manner by which AIMPAC corrects for this deviation is described in the Appendix.

1.8.6

Atomic Dipolar Polarization [$\mu(\Omega)$]

Also known as the *first atomic electrostatic moment*, atomic dipolar polarization is the atomic space average of the electronic position vector. It is a three-dimensional vector with components and magnitude defined in Eqs (38) and (39), respectively:

$$\boldsymbol{\mu}(\Omega) = \begin{pmatrix} \mu_x \\ \mu_y \\ \mu_z \end{pmatrix} = \begin{pmatrix} -e \int_{\Omega} x\rho(\mathbf{r}) d\mathbf{r} \\ -e \int_{\Omega} y\rho(\mathbf{r}) d\mathbf{r} \\ -e \int_{\Omega} z\rho(\mathbf{r}) d\mathbf{r} \end{pmatrix} \equiv -e \int_{\Omega} \mathbf{r}_{\Omega}\rho(\mathbf{r}) d\mathbf{r} \quad (38)$$

$$|\boldsymbol{\mu}(\Omega)| = \sqrt{\mu_x^2 + \mu_y^2 + \mu_z^2} \quad (39)$$

with the origin for the vector \mathbf{r}_{Ω} at the nucleus of atom Ω , i.e. $\mathbf{r}_{\Omega} = \mathbf{r} - \mathbf{R}_{\Omega}$, \mathbf{r} being the electronic coordinates and \mathbf{R}_{Ω} the nuclear coordinates of atom Ω . The first moment measures the polarization of the charge density, that is to say the departure from sphericity of the electron density.

The dipolar polarization can be used to understand the origins of permanent and induced molecular dipole moments and dielectric polarization in materials [55, 56]. Carbon monoxide is an instructive example [57]. The dipole moment of the CO molecule has the (unexpected) polarity $\delta^-C=O^{\delta+}$, opposite to intuition based on the relative electronegativities of carbon and oxygen. This observation is readily explained when one considers both atomic charges and atomic dipoles. Calculated atomic charges are indeed in accordance with the expected relative electronegativities of these two atoms (an electronegativity of 2.5 for carbon and

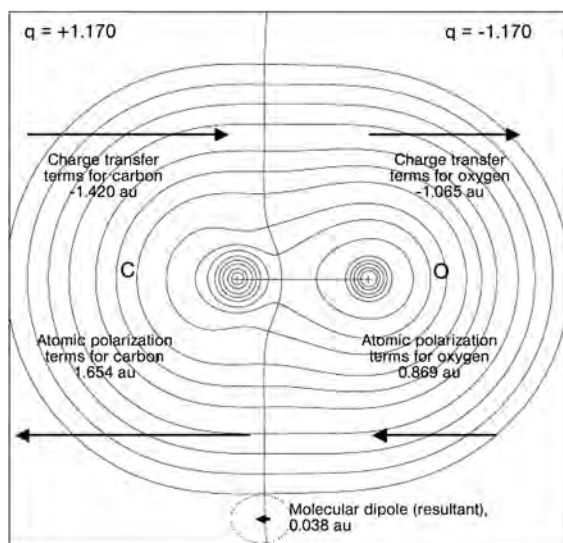


Fig. 1.5 Contour plot of the electron density of CO, showing the magnitudes and directions of atomic and charge-transfer dipoles (arrow lengths are proportional to the dipoles magnitudes). The head of an arrow points to the negative end of a dipole. The molecular dipole moment is given by the vector sum of the charge-transfer terms (μ_{CT})

and the atomic polarizations (μ_{AP}). The directly calculated SCF molecular dipole is 0.096 debyes (D) at the B3LYP/6-311+G(3df) and the corresponding dipole obtained from group contributions is 0.096 D, (experimental: 0.110 D). (Reproduced from Ref. [57] with the permission from the American Chemical Society).

3.5 for oxygen) [58] with the carbon bearing a positive charge [$q(C) = +1.17$ au] and the oxygen a negative charge, resulting in a *charge-transfer dipole* with the direction $^{+1.17}\text{C}=\overset{-1.17}{\text{O}}$. The electron density of each of the two atomic basins responds to this charge-transfer dipole with an opposing dipolar polarization $\overset{\leftarrow}{\text{C}}=\overset{\leftarrow}{\text{O}}$ with a magnitude which is not only sufficient to cancel the charge-transfer dipole but to slightly exceed it. The net result is a small dipole in complete accordance with the unexpected experimental result (Fig. 1.5). Thus, it is necessary to take the vectorial sum of both the charge transfer and the atomic polarization dipoles in defining atomic or group contributions to the molecular dipole moment [55, 56].

A program, FRAGDIP [59], is available for calculation of additive atomic and group contributions to the molecular dipole moment. As an illustration, Table 1.1 lists the group contributions to the dipole moments of several naturally occurring amino acids with their vector sum and compares this sum with the dipole moments calculated directly from an SCF calculation (second line). Each amino acid in its neutral form, with general formula $\text{R}-\text{CH}(\text{NH}_2)\text{COOH}$, was regarded as consisting of two groups – the side-chain (R-) and the “main chain” ($-\text{CH}(\text{NH}_2)\text{COOH}$). The reader can see how closely the group contributions sum to the molecular dipole.

Table 1.1 Comparison of the molecular dipole moments of some amino acids obtained from group contributions with those obtained directly from SCF calculations.^[a,b] The table also compares the second letter of the genetic code of each amino acid with side-chain dipole. (Adapted from Refs. [56, 60]).

Amino acid	Second base in the mRNA genetic codon ^[c]	Nature of the 2nd base ^[d] in the codon	Side-chain dipole ^[a,b] (au)			μ	Main-chain dipole ^[a,b] (au)			μ	Total molecular dipole ^[a,b] (au)			μ
			μ_x	μ_y	μ_z		μ_x	μ_y	μ_z		μ_x	μ_y	μ_z	
Gly	G	I	-0.006	0.068	-0.098	0.119	0.415	-0.376	0.095	0.568	0.409	-0.307	-0.002	0.512
Ile	U	II	0.130	0.012	-0.074	0.150	-0.363	0.521	-0.267	0.689	0.402	-0.317	-0.001	0.512
Ala	C	II	0.034	-0.108	-0.120	0.165	0.217	0.590	-0.073	0.632	-0.207	0.537	-0.269	0.635
Val	U	II	-0.103	0.149	-0.062	0.191	0.097	-0.621	-0.266	0.683	0.252	0.480	-0.193	0.576
Leu	U	II	0.069	0.182	0.081	0.211	-0.195	-0.607	0.163	0.658	-0.006	-0.473	-0.328	0.575
Phe	U	II	0.217	-0.142	-0.118	0.285	-0.099	0.642	-0.057	0.652	-0.013	-0.473	-0.319	0.571
Tyr	A	I	-0.292	-0.401	-0.201	0.536	0.138	-0.622	-0.065	0.641	-0.127	-0.424	0.244	0.506
											-0.119	-0.412	0.264	0.503
											0.118	0.501	-0.175	0.543
											0.077	0.495	-0.187	0.535
											-0.154	-1.024	-0.266	1.069
											-0.137	-1.026	-0.272	1.071
Thr	C	II	0.399	-0.259	-0.548	0.726	0.114	-0.645	0.065	0.658	0.514	-0.904	-0.483	1.147
											0.515	-0.904	-0.479	1.146
Met	U	II	-0.377	-0.636	-0.327	0.809	-0.288	-0.005	-0.382	0.479	-0.665	-0.642	-0.709	1.165
											-0.661	-0.647	-0.695	1.157

Trp	G	I	0.354	0.727	-0.140	0.820	-0.084	0.498	-0.173	0.534	0.270	1.225	-0.313	1.293
											0.245	1.233	-0.315	1.296
Cys	G	I	-0.692	0.090	0.450	0.830	-0.366	0.017	-0.479	0.603	-1.058	0.107	-0.029	1.064
											-1.047	0.118	-0.033	1.055
Ser	G/C ^e	I/II ^e	-0.823	-0.091	0.174	0.847	0.390	-0.428	-0.047	0.581	-0.433	-0.519	0.127	0.688
											-0.441	-0.528	0.130	0.700
Gln	A	I	-0.206	-1.296	-1.030	1.668	-0.056	0.436	0.695	0.823	-0.261	-0.860	-0.335	0.959
											-0.255	-0.894	-0.339	0.989
His	A	I	-1.510	-0.722	0.782	1.848	-0.380	0.097	-0.487	0.625	-1.890	-0.625	0.295	2.013
											-1.860	-0.637	0.303	1.989
Asn	A	I	-0.963	1.631	-0.197	1.904	-0.019	-0.651	-0.249	0.697	-0.982	0.980	-0.446	1.457
											-0.983	0.988	-0.458	1.467

^aThe total molecular dipole of an amino acid symbolized by R-CH(NH₂)COOH is given in the last four columns. For each amino acid, the top line in the last four columns lists the dipole moment obtained from the "side-chain" (R-) and the "main chain" (-CH(NH₂)COOH) group contributions using the FRAGDIP program [55, 56, 59], and the second line lists the corresponding dipole moment calculated directly from the SCF using the Gaussian program [61].

^bElectronic structure calculations were performed at the HF/6-311++G(d,p)//HF/6-31+G(d) level of theory.

^cThe second base in the RNA triplet genetic code of the amino acid: A = adenine, C = cytosine, G = guanine, U = uracil.

^dThe chemical nature of the second base in the triplet code: I = purine (adenine and guanine), and II = pyrimidine (cytosine, uracil).

^eSerine is the only amino acid which has a degenerate genetic code in the second position, all other amino acids have a unique base in the second position in all of their synonymous codons.

Further, the listings in Table 1.1 have been sorted in terms of the magnitude of the side-chain dipole magnitude, a sorting that reveals a striking regularity in the genetic code. Most amino acids listed in the upper part of the table with side-chain dipole magnitude less than 0.81 au (i.e. with non-polar side-chains) are encoded by a genetic triplet code having a pyrimidine base as the middle letter in the mRNA codon (except glycine, which lacks a side-chain, and tyrosine). On the other hand, most polar amino acids (having side-chain dipole magnitudes greater than 0.81 au) are encoded by a purine base, serine being the only “degenerate” amino acid, having codons of both types [56, 60]. Whereas this regularity in the genetic code has been well known for a long time, it is given a quantitative basis derived directly from the electron density distributions of the amino acids for the first time [60].

1.8.7

Atomic Quadrupolar Polarization $[\mathbf{Q}(\Omega)]$

The atomic quadrupolar polarization tensor is also known as the *second atomic electrostatic moment*. It is a symmetric traceless tensor defined as:

$$\mathbf{Q}(\Omega) = \begin{pmatrix} Q_{xx} & Q_{xy} & Q_{xz} \\ Q_{yx} & Q_{yy} & Q_{yz} \\ Q_{zx} & Q_{zy} & Q_{zz} \end{pmatrix} \\ \equiv -\frac{e}{2} \begin{pmatrix} \int_{\Omega} (3x_{\Omega}^2 - r_{\Omega})\rho(\mathbf{r}) \, d\mathbf{r} & 3 \int_{\Omega} x_{\Omega}y_{\Omega}\rho(\mathbf{r}) \, d\mathbf{r} & 3 \int_{\Omega} x_{\Omega}z_{\Omega}\rho(\mathbf{r}) \, d\mathbf{r} \\ 3 \int_{\Omega} y_{\Omega}x_{\Omega}\rho(\mathbf{r}) \, d\mathbf{r} & \int_{\Omega} (3y_{\Omega}^2 - r_{\Omega})\rho(\mathbf{r}) \, d\mathbf{r} & \int_{\Omega} y_{\Omega}z_{\Omega}\rho(\mathbf{r}) \, d\mathbf{r} \\ 3 \int_{\Omega} z_{\Omega}x_{\Omega}\rho(\mathbf{r}) \, d\mathbf{r} & \int_{\Omega} z_{\Omega}y_{\Omega}\rho(\mathbf{r}) \, d\mathbf{r} & \int_{\Omega} (3z_{\Omega}^2 - r_{\Omega})\rho(\mathbf{r}) \, d\mathbf{r} \end{pmatrix} \quad (40)$$

where, as for the first moment, the origin is placed at the nucleus. If the atomic electron density has spherical symmetry, then $\int_{\Omega} x_{\Omega}^2\rho(\mathbf{r}) \, d\mathbf{r} = \int_{\Omega} y_{\Omega}^2\rho(\mathbf{r}) \, d\mathbf{r} = \int_{\Omega} z_{\Omega}^2\rho(\mathbf{r}) \, d\mathbf{r} = \frac{1}{3} \int_{\Omega} r_{\Omega}^2\rho(\mathbf{r}) \, d\mathbf{r}$, and $Q_{xx} = Q_{yy} = Q_{zz} = 0$. Thus, the quadrupole moment is another measure of the deviation of the atomic electron density from spherical symmetry. For example, if a diagonal component of $\mathbf{Q}(\Omega)$ is <0 , the electron density is concentrated along that axis, and vice versa. It is always possible to find a coordinate system such that the original tensor in Eq. (40) $[\mathbf{Q}(\Omega)]$ is diagonalized $[\mathcal{Q}(\Omega)]$. The diagonalization of $\mathbf{Q}(\Omega)$ corresponds to a rotation of the original coordinate system. The diagonalized quadrupole tensor corresponding to Eq. (40) is written:

$$\mathcal{Q}(\Omega) = \begin{pmatrix} \mathcal{Q}_{x'x'} & 0 & 0 \\ 0 & \mathcal{Q}_{y'y'} & 0 \\ 0 & 0 & \mathcal{Q}_{z'z'} \end{pmatrix} \quad (41)$$

where $\mathcal{Q}_{x'x'}$, $\mathcal{Q}_{y'y'}$, and $\mathcal{Q}_{z'z'}$ are the principal values of the quadrupole moment with regard to the principal (rotated) axes, the x' , y' , and z' axes, which correspond to axes of symmetry if they exist in the electron density distribution (the primes will be dropped for simplicity).

The traceless property of the tensor defined in Eq. (40) (or in its diagonalized form, Eq. 41) is a consequence of the equality:

$$r_{\Omega}^2 = x_{\Omega}^2 + y_{\Omega}^2 + z_{\Omega}^2 \quad (42)$$

which is always true in any coordinate system. Therefore:

$$(Q_{xx} + Q_{yy} + Q_{zz}) = (\mathcal{Q}_{xx} + \mathcal{Q}_{yy} + \mathcal{Q}_{zz}) = 0 \quad (43)$$

and only five independent components completely specify $\mathbf{Q}(\Omega)$ in the original coordinate system and only two are sufficient to specify its diagonalized form $\mathcal{Q}(\Omega)$.

Finally, the magnitude of the quadrupolar polarization moment is defined as [62]:

$$|\mathbf{Q}| = \sqrt{\frac{2}{3}(Q_{xx}^2 + Q_{yy}^2 + Q_{zz}^2)} = \sqrt{\frac{2}{3}(\mathcal{Q}_{xx}^2 + \mathcal{Q}_{yy}^2 + \mathcal{Q}_{zz}^2)} \quad (44)$$

1.9

"Practical" Uses and Utility of QTAIM Bond and Atomic Properties

1.9.1

The Use of QTAIM Bond Critical Point Properties

Several QTAIM bond properties have been shown to be correlated with experimental molecular properties. For example, the electron density at the BCP, ρ_b , has been shown on several occasions to be strongly correlated with the bond energies, and hence provide a measure of bond order (Eq. 8) [1, 30]; the potential energy density at the BCP has been shown to be highly correlated with hydrogen bond energies [32]; full interaction potentials in hydrogen bonds were recovered from the potential energy density at the BCP [63]; π - π stacking interactions in benzene dimers and in stacked DNA bases and base-pairs have been found to be highly correlated to BCP and cage critical point data between π -stacked monomers [64–66].

The use of BCP properties in drug design is a field pioneered by Popelier and coworkers. These authors proposed the construction of a vector space from bond properties evaluated at the bond critical points, i.e. a point in this space is specified by a set of bond properties [67–70]. This space was used as a basis for comparing related molecules, the smaller the distance between two molecules in this

space the more they are similar. Quantification of molecular similarity in this manner has several advantages over other similarity measures (for example Carbo's similarity index [71]):

1. it is much faster because it involves no spatial integration (the density of each molecule is only sampled at the positions of the BCPs);
2. it is not dominated by nuclear maxima but rather emphasizes the more interesting chemical bonding regions of the molecule; and
3. it is not plagued with the alignment problem, in which one must often choose how to align the molecules to be compared before the integration.

The new method has been successful in accurately predicting a number of properties of several series of molecules [67–70].

1.9.2

The Use of QTAIM Atomic Properties

The review in this section follows closely Table 1 of Ref. [51].

Atomic properties have been used to recover and *directly* predict several experimentally additive atomic and group contributions to molecular properties, including, for example, heats of formation [72], magnetic susceptibility (Refs [73–77] and Chapter 3 in this book), molecular volumes [78], electric moments (Chapter 3) and polarizability [79–81], Raman intensities [79, 81–84] (see also Chapter 4), IR intensities [85–88] (see also Chapter 4), spectroscopic transition probabilities [89], dielectric polarization in crystals and molecular dipole and quadrupole moments [55, 90, 91], Wigner–Seitz cells in crystals [92], group additivity in silanes [93], and Pascal's aromatic exaltations [1]. They have also been used to provide an atomic basis for electron localization and delocalization [42, 43, 47, 94, 95].

Atomic properties have also been used *empirically* to predict several experimental properties including for example, the pK_a of weak acids from the atomic energy of the acidic hydrogen [96], a wide array of biological and physicochemical properties of the amino acids, including the genetic code itself, and the effects of mutation on protein stability [60], protein retention times [97], HPLC column capacity factors of high-energy materials [98], NMR spin–spin coupling constants from the electron delocalization indices [99, 100], simultaneous consistent prediction of five bulk properties of liquid HF in MD simulation [101], classification of atom types in proteins with future potential applications in force-field design [60, 102–104], reconstructing large molecules from transferable fragments or atoms in molecules [60, 105–119] (see also Chapters 11 and 12), atomic partitioning of the molecular electrostatic potential [120–122], prediction of hydrogen-bond donor capacity [123] and basicity [124], and to provide an atomic basis for curvature-induced polarization in carbon nanotubes and nanoshells [125].

1.10 Steps of a Typical QTAIM Calculation

It should be clear from the outset that QTAIM applies equally well to experimental [2, 126] and calculated electron densities [1, 3]; in this tutorial, however, we will discuss calculated densities.

The starting point for the application of the QTAIM theory is the electron density. The density can be calculated from the many-electron single-determinant or many-determinant wavefunction (or Slater-like determinants built from Kohn–Sham orbitals in density functional theory [127]) obtained by a variety of methods and software. The electron density necessary for meaningful analysis by means of QTAIM must be obtained with a basis set flexible enough for an accurate representation of the bonding regions, in other words it must include polarization functions. In the case of anions, excited states, and weak bonding interactions between atoms separated by relatively large distances one must augment the basis set with diffuse functions. When heavy atoms are present in the molecule, which usually necessitates the use of effective core potentials (ECP), it is necessary to treat the valence shell and at least one sub-valence shell explicitly to obtain meaningful results from the integrations. It is important to note that bond paths cannot be traced to the nuclei of atoms described by ECPs. Alternatively, often the geometry is optimized with a basis set including the ECP on the heavy atoms followed by a single point calculation at the optimized geometry using a full basis set on all atoms.

The first step in a molecular QTAIM calculation is, thus, the generation of a wavefunction (or wavefunction-like single determinant in a DFT calculation [127]) from an electronic structure calculation with software such as Gaussian [61] or GAMESS [128].

The electron density derived from the wavefunction is then subjected to a point-by-point topological analysis to locate the bond critical points and the bond paths, by use of software such as EXTREME [129–131]. The space of the molecule is then partitioned by the zero-flux surfaces and atomic integrations are performed to obtain the atomic contributions to the molecular properties using software such as PROAIM and its variants [129–131]. EXTREME and PROAIM are both part of the AIMPAC suite of programs developed in Professor Bader’s laboratory (*McMaster University*) [129–131].

Several other software packages derived from AIMPAC are available for analysis of the electron density according to QTAIM. Among the widely used programs are MORPHY [132], developed by Dr Paul Popelier’s group (*University of Manchester*), and AIM2000 [133–135], developed by Professor Friederich Biegler-König (*University of Bielefeld*), both of which apply to molecular calculations. The program TOPOND [136] (described in Chapter 7) was developed by Dr Carlo Gatti (*National Research Council of Italy*) for the analysis of periodic densities obtained from CRYSTAL [137].

After all atomic integrations have been performed to the desired accuracy (as measured by the value of the integrated Laplacian) one typically uses shell scripts

and/or simple UNIX/Linux commands such as “grep” to extract the relevant information from the electronic integration files. In this manner the summarized results can be further imported to a spreadsheet or a plotting program. Integration files – which contain the atomic overlap matrices – can be subsequently analyzed by software such as AIMDELOC [44] or LI-DICALC [45, 46] to obtain the localization and delocalization indices.

Further, the wavefunction files can be used as input to plotting routines. GRDVEC can be used to generate two-dimensional plots of the gradient vector field and/or the interatomic surfaces and bond paths projected on a plane selected by the user (right half of Fig. 1.3a). Contour diagrams of the density (such as those in the left half of Fig. 1.3a, and Fig. 1.5), the Laplacian, or energy densities can be generated by first calculating the corresponding grid by the use of GRIDV software followed by the generation of the graphics file from the grid

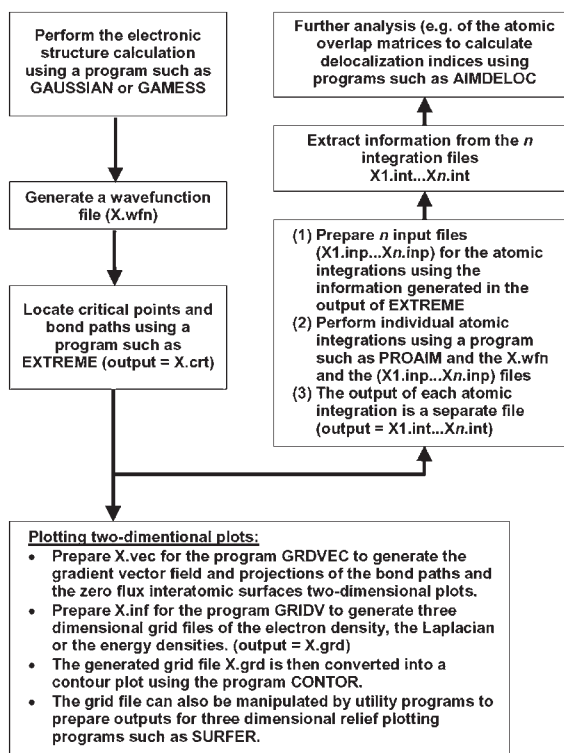


Fig. 1.6 The main steps in a simple QTAIM calculation. The software cited in the figure is part of the AIMPACK suite of programs [129–131]. Other programs are available that can perform most or all of these steps, including, for example, AIM2000 [133–135], MORPHY [132], and AIMALL97 [139].

by using a program such as CONTOR. (GRDVEC, GRIDV, and CONTOR are components of AIMPAC [129–131]).

The grid generated by GRIDV can be manipulated by utility programs such as GridV_REFORMATTER (available from the authors) to generate inputs for programs such as Surfer [138] which produce three-dimensional relief maps of the field represented by the calculated grid (Fig. 1.1b is an example).

The main steps of a typical QTAIM calculation are summarized in Fig. 1.6.

Appendix: The Inexact Satisfaction of the Molecular Virial Theorem in Electronic Structure Calculations

For a molecule in an equilibrium geometry (with vanishing forces on the nuclei), the molecular virial theorem is expressed as:

$$\gamma = -\frac{V}{T} = 2 \quad (45)$$

Because of the propagation of numerical errors, small (but non-vanishing) thresholds of convergence of both the SCF and the geometry optimization steps, and the use of incomplete basis sets, electronic structure calculations do not usually satisfy the virial theorem exactly and the virial ratio (γ) can deviate by perhaps as much as 0.01 from the ideal value of 2. As a result of this deviation, atomic energies will not sum to yield the molecular energy with acceptable accuracy.

Atomic integration software such as PROAIM [129–131] correct for this error numerically. Thus, instead of simply multiplying each atomic kinetic energy $T(\Omega)$ by (-1) to obtain the total atomic energy $E(\Omega)$, the latter is obtained by multiplying $T(\Omega)$ by $(1 - \gamma)$. These corrected atomic energies do satisfy Eq. (37), and their sum equals the total molecular energy to within a small numerical *integration* error. The virial corrections usually scale linearly with regard to $T(\Omega)$ which, fortunately, leaves the relative stabilities of the atoms unchanged.

The integration software obtains the virial ratio from the wavefunction files generated by Gaussian [61] or GAMESS [128]. The virial is printed in the last line in the wavefunction file. For Hartree–Fock or density functional calculations, Gaussian prints the correct virial in the wavefunction file and the integrations proceed without problems. For wavefunction files calculated at a post Hartree–Fock level, for example those obtained using Møller–Plesset perturbation theory (MP n) or configuration interaction methods (CI), the virial printed in the wavefunction file generated using the Gaussian 98 or 03 [61] programs (which are available at the time of writing) is *the Hartree–Fock virial and not that of the current post-Hartree–Fock method* [even if the key word “DENSITY = CURRENT” is invoked and despite the fact that the correct (current) wavefunction is printed]. If such a wavefunction file is fed directly to an integration program, the calculated atomic energies will be rectified using the Hartree–Fock γ (instead of the post Hartree–Fock γ), resulting in atomic energies which do not add up to the molecular value.

In these circumstances the user must calculate the virial of the current method “by hand” from information contained in the Gaussian “log” or “out” output file [140], by dividing, for example, the MP2 (or other correlated total energy) by the kinetic energy listed just after the final electrical multipoles in the Gaussian output. The wavefunction files must then be edited to reflect this new “correct” virial before submitting it to the integration software [140].

In highly accurate calculations it is sometimes necessary to perform atomic integrations of energy densities obtained from systems which satisfy the molecular virial theorem exactly [16, 141]. The author of Chapter 3 of this book, Dr Todd A. Keith, has written a link [142] for Gaussian [61] implementing Löwdin’s self-consistent virial scaling (SCVS) [143, 144] which produces final wavefunctions satisfying the virial theorem to a very high accuracy.

Acknowledgments

We thank Professor George Heard (University of North Carolina at Asheville) and Dr Katherine N. Robertson (Dalhousie University) for their helpful comments on this chapter, and Dr Todd Keith (Semichem, Inc.) and Dr Jamie Platts (Cardiff University) for discussions on the virial correction. The American Chemical Society is acknowledged for its permission to reproduce Fig. 1.5.

References

- 1 R. F. W. Bader, *Atoms in Molecules: A Quantum Theory*, Oxford University Press: Oxford, U.K., 1990.
- 2 P. Coppens, *X-ray Charge Densities and Chemical Bonding*, Oxford University Press, Inc.: New York, 1997.
- 3 P. L. A. Popelier, *Atoms in Molecules: An Introduction*, Prentice Hall: London, 2000.
- 4 C. F. Matta, N. Castillo, R. J. Boyd, *J. Phys. Chem. A* **2005**, *109*, 3669–3681.
- 5 N. Castillo, C. F. Matta, R. J. Boyd, *Chem. Phys. Lett.* **2005**, *409*, 265–269.
- 6 C. Gatti, P. Fantucci, G. Pacchioni, *Theor. Chem. Acc. (Formerly, Theoret. Chim. Acta)* **1987**, *72*, 433–458.
- 7 W. L. Cao, C. Gatti, P. J. MacDougall, R. F. W. Bader, *Chem. Phys. Lett.* **1987**, *141*, 380–385.
- 8 M. Sakata, *Acta Cryst. A* **1990**, *46*, 263–270.
- 9 R. Y. de Vries, W. J. Briels, D. Feil, G. te Velde, E. J. Baerends, *Can. J. Chem.* **1996**, *74*, 1054–1058.
- 10 A. Taylor, C. F. Matta, R. J. Boyd, submitted for publication **2006**.
- 11 R. F. W. Bader, J. A. Platts, *J. Chem. Phys.* **1997**, *107*, 8545–8553.
- 12 R. F. W. Bader, *Phys. Rev. B* **1994**, *49*, 13348–13356.
- 13 J. Schwinger, *Phys. Rev.* **1951**, *82*, 914–927.
- 14 R. F. W. Bader, *J. Phys. Chem. A* **1998**, *102*, 7314–7323.
- 15 T. A. Keith, R. F. W. Bader, Y. Aray, *Int. J. Quantum Chem.* **1996**, *57*, 183–198.
- 16 C. F. Matta, J. Hernández-Trujillo, T. H. Tang, R. F. W. Bader, *Chem. Eur. J.* **2003**, *9*, 1940–1951.
- 17 C. F. Matta, Chapter 9 in: *Hydrogen Bonding – New Insight*, (S. J. Grabowski, Ed.), Springer: 2006, pp 337–376.
- 18 R. F. W. Bader, C. F. Matta, *J. Phys. Chem. A* **2004**, *108*, 8385–8394.
- 19 R. P. Sagar, A. C. T. Ku, V. H. Jr. Smith, A. M. Simas, *J. Chem. Phys.* **1988**, *88*, 4367–4374.

- 20 Z. Shi, R. J. Boyd, *J. Chem. Phys.* **1988**, *88*, 4375–4377.
- 21 R. W. F. Bader, G. L. Heard, *J. Chem. Phys.* **1999**, *111*, 8789–8797.
- 22 R. J. Gillespie, R. S. Nyholm, *Quart. Rev. Chem. Soc.* **1957**, *11*, 339.
- 23 R. J. Gillespie, R. S. Nyholm, in: *Progress in Stereochemistry* (W. Klyne, P. B. D. de la Mare, Eds.), Butterworths: London, 1958.
- 24 R. J. Gillespie, I. Hargittai, *The VSEPR Model of Molecular Geometry*, Allyn and Bacon: Boston, 1991.
- 25 R. F. W. Bader, P. J. MacDougall, C. D. H. Lau, *J. Am. Chem. Soc.* **1984**, *106*, 1594–1605.
- 26 R. F. W. Bader, R. J. Gillespie, P. J. MacDougall, *J. Am. Chem. Soc.* **1988**, *110*, 7329–7336.
- 27 R. J. Gillespie, I. Bytheway, T.-H. Tang, R. F. W. Bader, *Inorg. Chem.* **1996**, *35*, 3954–3963.
- 28 M. T. Carroll, C. Chang, R. F. W. Bader, *Mol. Phys.* **1988**, *63*, 387–405.
- 29 M. T. Carroll, J. R. Cheeseman, R. Osman, H. Weinstein, *J. Phys. Chem.* **1989**, *93*, 5120–5123.
- 30 R. J. Boyd, S. C. Choi, *Chem. Phys. Lett.* **1986**, *129*, 62–65.
- 31 M. T. Carroll, R. F. W. Bader, *Mol. Phys.* **1988**, *65*, 695–722.
- 32 E. Espinosa, E. Molins, C. Lecomte, *Chem. Phys. Lett.* **1998**, *285*, 170–173.
- 33 S. J. Grabowski, *J. Phys. Chem. A* **2001**, *105*, 10739–10746.
- 34 M. Domagala, S. Grabowski, K. Urbaniak, G. Mloston, *J. Phys. Chem. A* **2003**, *107*, 2730–2736.
- 35 S. Grabowski, W. A. Sokalski, J. Leszczynski, *J. Phys. Chem. A* **2005**, *109*, 4331–4341.
- 36 M. Domagala, S. Grabowski, *J. Phys. Chem. A* **2005**, *109*, 5683–5688.
- 37 O. Knop, R. J. Boyd, S. C. Choi, *J. Am. Chem. Soc.* **1988**, *110*, 7299–7301.
- 38 J. L. Jules, J. R. Lombardi, *J. Mol. Struct. (Theochem)* **664–665**, *2003*, 255–271.
- 39 S. T. Howard, O. Lamarche, *J. Phys. Org. Chem.* **2003**, *16*, 133–141.
- 40 R. F. W. Bader, T. T. Nguyen-Dang, *Adv. Quantum Chem.* **1981**, *14*, 63–124.
- 41 D. Cremer, E. Kraka, *Angew. Chem. Int. Ed. Engl.* **1984**, *23*, 627–628.
- 42 X. Fradera, M. A. Austen, R. F. W. Bader, *J. Phys. Chem. A* **1999**, *103*, 304–314.
- 43 R. F. W. Bader, M. E. Stephens, *J. Am. Chem. Soc.* **1975**, *97*, 7391–7399.
- 44 C. F. Matta, *AIMDELOC (QCPE 0802)* Quantum Chemistry Program Exchange, Indiana University, 2001. (<http://qcpe.chem.indiana.edu/>).
- 45 Y.-G. Wang, C. F. Matta, N. H. Werstiuk, *J. Comput. Chem.* **2003**, *24*, 1720–1729.
- 46 Y.-G. Wang, N. H. Werstiuk, *J. Comput. Chem.* **2003**, *24*, 379–385.
- 47 M. A. Austen, *A New Procedure for Determining Bond Orders in Polar Molecules, with Applications to Phosphorus and Nitrogen Containing Systems*, Ph.D. Thesis, McMaster University: Hamilton, Canada, 2003.
- 48 C. F. Matta, J. Hernández-Trujillo, *J. Phys. Chem. A* **2003**, *107*, 7496–7504 (Correction: *J. Phys. Chem. A* **2005**, *109*, 10798).
- 49 E. A. Zhurova, C. F. Matta, N. Wu, V. V. Zhurov, A. A. Pinkerton, *J. Am. Chem. Soc.* **2006**, *128*, 8849–8861.
- 50 R. F. W. Bader, P. F. Zou, *Chem. Phys. Lett.* **1992**, *191*, 54–58.
- 51 C. F. Matta, R. F. W. Bader, *J. Phys. Chem. A* **2006**, *110*, 6365–6371.
- 52 (a) L. Cohen, *J. Chem. Phys.* **1979**, *70*, 788–789; (b) L. Cohen, *J. Chem. Phys.* **1984**, *80*, 4277–4279.
- 53 F. Cortés-Guzmán, J. Hernández-Trujillo, G. Cuevas, *J. Phys. Chem. A* **2003**, *107*, 9253–9256.
- 54 R. F. W. Bader, J. R. Cheeseman, K. E. Laidig, K. B. Wiberg, C. Breneman, *J. Am. Chem. Soc.* **1990**, *112*, 6530–6536.
- 55 R. F. W. Bader, C. F. Matta, *Int. J. Quantum Chem.* **2001**, *85*, 592–607.
- 56 C. F. Matta, *Applications of the Quantum Theory of Atoms in Molecules to Chemical and Biochemical Problems*, Ph.D. Thesis, McMaster University: Hamilton, Canada, 2002. (Available on line, <http://chem.utoronto.ca/~cmatta/>).
- 57 C. F. Matta, R. J. Gillespie, *J. Chem. Educ.* **2002**, *79*, 1141–1152.

- 58 L. Pauling, *The Nature of the Chemical Bond*, (Third Ed.), Cornell University Press: Ithaca, N.Y., 1960.
- 59 C. F. Matta, *FRAGDIP (QCPE 0801)* Quantum Chemistry Program Exchange, Indiana University, 2001. (<http://qcpe.chem.indiana.edu/>).
- 60 C. F. Matta, R. F. W. Bader, *Proteins: Struct. Funct. Genet.* **2003**, *52*, 360–399.
- 61 M. J. Frisch, *et al.*, Gaussian 03, Gaussian Inc.: Pittsburgh PA, 2003.
- 62 C. G. Gray, K. E. Gubbins, *Theory of Molecular Fluids*, (Vol. 1), Clarendon Press: Oxford, 1984.
- 63 E. Espinosa, E. Molins, *J. Chem. Phys.* **2000**, *113*, 5686–5694.
- 64 O. A. Zhikol, O. Shishkin, K. A. Lyssenko, J. Leszczynski, *J. Chem. Phys.* **2005**, *122*, 144104-1–144104-8.
- 65 M. P. Waller, A. Robertazzi, J. A. Platts, D. E. Hibbs, P. A. Williams, *J. Comput. Chem.* **2006**, *27*, 491–504.
- 66 C. F. Matta, N. Castillo, R. J. Boyd, *J. Phys. Chem. B* **2006**, *110*, 563–578.
- 67 S. E. O'Brien, P. L. A. Popelier, *Can. J. Chem.* **1999**, *77*, 28–36.
- 68 P. L. A. Popelier, *J. Phys. Chem. A* **1999**, *103*, 2883–2890.
- 69 S. E. O'Brien, P. L. A. Popelier, *J. Chem. Inf. Comput. Sci.* **2001**, *41*, 764–775.
- 70 U. A. Chaudry, P. L. A. Popelier, *J. Org. Chem.* **2004**, *69*, 233–241.
- 71 R. Carbó, L. Leyda, M. Arnau, *Int. J. Quantum Chem.* **1980**, *17*, 1185–1189.
- 72 K. B. Wiberg, R. F. W. Bader, C. D. H. Lau, *J. Am. Chem. Soc.* **1987**, *109*, 1001–1012.
- 73 T. A. Keith, R. F. W. Bader, *Chem. Phys. Lett.* **1992**, *194*, 1–8.
- 74 T. A. Keith, R. F. W. Bader, *Int. J. Quantum Chem.* **1996**, *60*, 373–379.
- 75 R. F. W. Bader, T. A. Keith, *J. Chem. Phys.* **1993**, *99*, 3683–3693.
- 76 T. A. Keith, R. F. W. Bader, *Chem. Phys. Lett.* **1993**, *210*, 223–231.
- 77 T. A. Keith, R. F. W. Bader, *J. Chem. Phys.* **1993**, *99*, 3669–3682.
- 78 R. F. W. Bader, M. T. Carroll, J. R. Cheeseman, C. Chang, *J. Am. Chem. Soc.* **1987**, *109*, 7968–7979.
- 79 R. F. W. Bader, T. A. Keith, K. M. Gough, K. E. Laidig, *Mol. Phys.* **1992**, *75*, 1167–1189.
- 80 K. E. Laidig, *Can. J. Chem.* **1996**, *74*, 1131–1138.
- 81 K. M. Gough, M. M. Yacowar, R. H. Cleve, J. R. Dwyer, *Can. J. Chem.* **1996**, *74*, 1139–1144.
- 82 K. M. Gough, H. K. Srivastava, K. Belohorcová, *J. Chem. Phys.* **1993**, *98*, 9669–9677.
- 83 K. M. Gough, H. K. Srivastava, K. Belohorcová, *J. Phys. Chem.* **1994**, *98*, 771–776.
- 84 K. M. Gough, H. K. Srivastava, *J. Phys. Chem.* **1996**, *100*, 5210–5216.
- 85 R. L. A. Haiduke, A. E. de Oliveira, R. E. Bruns, *J. Phys. Chem. A* **2004**, *108*, 6788–6796.
- 86 J. V. da Silva, R. L. A. Haiduke, R. E. Bruns, *J. Phys. Chem. A* **2006**, *110*, 4839–4845.
- 87 P. H. César, S. H. D. M. Faria, J. V. da Silva Jr., R. L. A. Haiduke, R. E. Bruns, *Chem. Phys.* **2005**, *317*, 35–42.
- 88 R. L. A. Haiduke, R. E. Bruns, *J. Phys. Chem. A* **2005**, *109*, 2680–2688.
- 89 R. F. W. Bader, D. Bayles, G. L. Heard, *J. Chem. Phys.* **2000**, *112*, 10095–10105.
- 90 K. E. Laidig, *Chem. Phys. Lett.* **1991**, *185*, 483–489.
- 91 R. F. W. Bader, *Mol. Phys.* **2002**, *100*, 3333–3344.
- 92 P. F. Zou, R. F. W. Bader, *Acta Cryst. A* **1994**, *50*, 714–725.
- 93 R. F. W. Bader, D. Bayles, *J. Phys. Chem. A* **2000**, *104*, 5579–5589.
- 94 R. F. W. Bader, A. Streitwieser, A. Neuhaus, K. E. Laidig, P. Speers, *J. Am. Chem. Soc.* **1996**, *118*, 4959–4965.
- 95 R. F. W. Bader, S. Johnson, T.-H. Tang, P. L. A. Popelier, *J. Phys. Chem.* **1996**, *100*, 15398–15415.
- 96 K. R. Adam, *J. Phys. Chem. A* **2002**, *106*, 11963–11972.
- 97 M. Song, C. M. Breneman, J. Bi, N. Sukumar, K. P. Bennett, S. Cramer, N. Tugcu, *J. Chem. Inf. Comput. Sci.* **2002**, *42*, 1347–1357.
- 98 C. M. Breneman, M. Rhem, *J. Comput. Chem.* **1997**, *18*, 182–197.
- 99 C. F. Matta, J. Hernández-Trujillo, R. F. W. Bader, *J. Phys. Chem. A* **2002**, *106*, 7369–7375.

- 100 N. Castillo, C. F. Matta, R. J. Boyd, *J. Chem. Inf. Mod.* **2005**, *45*, 354–359.
- 101 S. Y. Liem, P. L. A. Popelier, *J. Chem. Phys.* **2003**, *119*, 4560–4566.
- 102 H. J. Bohórquez, M. Obregón, C. Cárdenas, E. Llanos, C. Suárez, J. L. Villaveces, M. E. Patarroyo, *J. Phys. Chem. A* **2003**, *107*, 10090–10097.
- 103 P. L. A. Popelier, F. M. Aicken, *ChemPysChem* **2003**, *4*, 824–829.
- 104 P. L. A. Popelier, F. M. Aicken, *J. Am. Chem. Soc.* **2003**, *125*, 1284–1292.
- 105 C. Chang, R. F. W. Bader, *J. Phys. Chem.* **1992**, *96*, 1654–1662.
- 106 C. M. Breneman, T. R. Thompson, M. Rhem, M. Dung, *Comput. Chem.* **1995**, *19*, 161–179.
- 107 C. M. Breneman, L. W. Weber, in: *The application of charge density research to chemistry and drug design (NATO ASI Series)*, (G. A. Jeffrey, J. F. E. Piniella, Eds.) Plenum Press, New York, 1991, pp 357–358.
- 108 C. F. Matta, R. F. W. Bader, *Proteins: Struct. Funct. Genet.* **2000**, *40*, 310–329.
- 109 C. F. Matta, R. F. W. Bader, *Proteins: Struct. Funct. Genet.* **2002**, *48*, 519–538.
- 110 R. F. W. Bader, F. J. Martín, *Can. J. Chem.* **1998**, *76*, 284–291.
- 111 F. J. Martín, *Theoretical Synthesis of Macromolecules from Transferable Functional Groups*, Ph.D. Thesis, McMaster University: Hamilton, 2001.
- 112 R. F. W. Bader, C. F. Matta, F. J. Martín, Chapter 7 in: *Medicinal Quantum Chemistry*, (F. Alber, P. Carloni, Eds.) Wiley–VCH: Weinheim, 2003, pp 201–231.
- 113 V. Pichon-Pesme, C. Lecomte, R. Wiest, M. Bénard, *J. Am. Chem. Soc.* **1992**, *114*, 2713–2715.
- 114 R. Wiest, V. Pichon-Pesme, M. Bénard, C. Lecomte *J. Phys. Chem.* **1994**, *98*, 1351–1362.
- 115 V. Pichon-Pesme, C. Lecomte, H. Lachekar, *J. Phys. Chem.* **1995**, *99*, 6242–6250.
- 116 C. Jelsch, V. Pichon-Pesme, C. Lecomte, A. Aubry, *Acta Cryst. D* **1998**, *54*, 1306–1318.
- 117 C. F. Matta, *J. Phys. Chem. A* **2001**, *105*, 11088–11101.
- 118 B. Dittrich, T. Koritsánszky, M. Grosche, W. Scherer, R. Flaig, A. Wagner, H. G. Krane, H. Kessler, C. Riemer, A. M. M. Schreurs, P. Luger, *Acta Cryst. B* **2002**, *58*, 721–727.
- 119 S. Scheins, M. Messerschmidt, P. Luger, *Acta Cryst. B* **2005**, *61*, 443–448.
- 120 D. S. Kosov, P. L. A. Popelier, *J. Chem. Phys.* **2000**, *113*, 3969–3974.
- 121 D. S. Kosov, P. L. A. Popelier, *J. Phys. Chem. A* **2000**, *104*, 7339–7345.
- 122 P. L. A. Popelier, L. Joubert, D. S. Kosov, *J. Phys. Chem. A* **2001**, *105*, 8254–8261.
- 123 J. A. Platts, *Phys. Chem. Chem. Phys.* **2000**, *2*, 973–980.
- 124 J. A. Platts, *Phys. Chem. Chem. Phys.* **2000**, *2*, 3115–3120.
- 125 T. Dumitrica, C. M. Landis, B. I. Yakobson, *Chem. Phys. Lett.* **2002**, *360*, 182–188.
- 126 T. S. Koritsánszky, P. Coppens, *Chem. Rev.* **2001**, *101*, 1583–1628.
- 127 W. Koch, M. C. Holthausen, *A Chemist's Guide to Density Functional Theory, (Second Edition)*, Wiley–VCH: New York, 2001.
- 128 M. W. Schmidt, K. K. Baldrige, J. A. Boatz, S. T. Elbert, M. S. Gordon, J. H. Jensen, S. Koseki, N. Matsunaga, K. A. Nguyen, S. J. Su, T. L. Windus, M. Dupuis, J. A. Montgomery, *J. Comput. Chem.* **1993**, *14*, 1347–1363.
- 129 Bader, R. F. W., <http://www.chemistry.mcmaster.ca/aimpac/>.
- 130 F. W. Biegler-König, T. T. Nguyen-Dang, Y. Tal, R. F. W. Bader, A. J. Duke *J. Phys. B: At. Mol. Phys.* **1981**, *14*, 2739–2751.
- 131 F. W. Biegler-König, R. F. W. Bader, T.-H. Tang, *J. Comput. Chem.* **1982**, *13*, 317–328.
- 132 Popelier, P. L. A., MORPHY, UMIST, England, EU, **1998**.
- 133 F. W. Biegler-König, J. Schönbohm, D. Bayles, *J. Comput. Chem.* **2001**, *22*, 545–559.
- 134 F. W. Biegler-König, *J. Comput. Chem.* **2000**, *21*, 1040–1048.

- 135 F. W. Biegler-König, J. Schönbohm, D. Bayles, AIM2000 Website: <http://gauss.fh-bielefeld.de/aim2000>.
- 136 C. Gatti, TOPOND, CNR-CSR SRC: Milano, 1998.
- 137 V. R. Saunders, R. Dovesi, C. Roetti, R. Orlando, C. M. Zicovich-Wilson, N. M. Harrison, K. Doll, B. Civalleri, I. J. Bush, Ph. D'Arco, M. Llunell, CRYSTAL 2003.
- 138 Surfer 08, Golden Software, Inc., Golden, Colorado, USA, 2002.
- 139 T. A. Keith, *AIMALL97 for Windows*, 1997.
- 140 J. A. Platts, CCL: MP2 virial value (8 July 2005), <http://www.ccl.net/cgi-bin/ccl/message.cgi?2005+07+08+004>.
- 141 F. Cortés-Guzmán, R. F. W. Bader, *Chem. Phys. Lett.* **2003**, 379, 183–192.
- 142 T. A. Keith, Link for self-consistent virial scaling (SCVS) in Gaussian 94/98, **1998**.
- 143 P.-O. Löwdin, *J. Mol. Spectr.* **1959**, 3, 46–66.
- 144 D. E. Magnoli, J. R. Murdoch, *Int. J. Quantum Chem.* **1982**, 22, 1249–1262.

Index

a

- ab initio wavefunction 86
- ab initio periodic approaches 169
- Abramov functional 432
- Abramov energy density 432
- absolute hardness 400
- absorption intensity 79
- accuracy of atomic integrations 17, 18
- acenaphthylene 408
- acetamide 333
- acrolein 129, 135, 136
- action integral 41
- action principle 39, 40, 44
- active site 511
- additivity of the atomic energy 10
- adenine 312
- adenine binding site 305 ff., 308, 312, 313
- adenine binding site of the protein hAR 302, 303, 310
- adenosine 323
- ADI 405, 406
- agostic interaction 364, 366, 367, 512
- agostic systems 365
- AIM2000 27, 101, 103 ff.
- AIMALL97 28
- AIMDELOC 15, 28
- AIMPAC 27, 29, 264
- Al 216
- Al₂C₂H₁₀ 145
- Al–Al bond 211
- aliphatic hydrocarbons 379
- alkali halides 214
- alkali metal clusters 192
- alkaline-earth metals 214
- alkane 77, 91, 109, 116 f.
- n*-alkanes 99
- n*-alkenes 194
- alkyne 114
- amino acid 21, 22, 24, 301, 324, 325
- amino acid residues 56, 285, 302, 303, 327
- ammonia 276
- analytical CPHF method 101
- anharmonicity 98
- anomeric effect 375, 386
- anthracene 408
- aromatic compounds 399
- aromatic radicals 393
- aromatic stabilization energy 400
- aromatic transition state (TS) 418
- aromatic π -sextets 416
- aromaticity 394, 395, 399
 - indices 394, 418 f.
- asphericity shifts 334
- atom types in proteins 26
- atomic additivity schemes 82
- atomic basin 6, 211, 428
 - shape 209 ff.
 - volume 16, 295
- atomic charge 9, 16, 75, 328, 401
 - derivatives 80, 81
 - transfer derivatives 80
 - transfer dipole contribution 75
- atomic components 176
- atomic continuity theorem 51
- atomic contributions 50, 62, 65, 71, 73, 74, 76, 81, 90 ff., 108
 - to $\bar{\alpha}$ 112
 - to $\Delta\bar{\alpha}/\Delta r_{\text{CH}}$ 112
 - to the electronic energy 18 ff., 276
 - to the magnetizability tensors 91
 - to the polarizability tensors 77
- atomic current theorem 51, 52
- atomic dipolar polarization 20
 - contribution 72
 - gradient 75
- atomic dipoles 109
- atomic electric polarizability tensors 91

- atomic electron populations 16, 103, 175, 277, 401
 - atomic electronic energy 19, 84
 - atomic electronic kinetic energy 17, 82
 - atomic electronic virial theorem 19, 83
 - atomic electrostatic multipole moments 20–25, 126
 - atomic energy XXII, 20, 29, 84
 - atomic exchange matrices 138
 - atomic force
 - microscope 54
 - theorem 51
 - atomic fragments 317
 - atomic graph 348
 - atomic group source function 195
 - atomic interaction lines 8
 - atomic interactions 260, 347
 - atomic magnetic polarization contribution 88
 - atomic multipolar ED 296
 - atomic multipole moments 20–25, 126
 - atomic multipoles model 122
 - atomic net charges 16, 188, 295, 299
 - atomic net current contribution 88
 - atomic nuclear virial energy 82 ff., 85
 - atomic polarizability 77
 - atomic polarization 20–25, 78, 80
 - atomic populations *see* atomic electron population
 - atomic power theorem 51
 - atomic properties 15–25, 26, 194
 - atomic quadrupolar polarization 24
 - atomic quadrupole moment 24, 175, 352
 - atomic source contributions in $\text{Mn}_2(\text{CO})_{10}$ 200
 - atomic surface derivative contributions 76
 - atomic theorems 51
 - atomic torque theorem 51
 - atomic virial theorem XXII, 19, 51
 - atomic volume 16, 277, 328, 352
 - attraction (repulsion) basin 210
 - Au (111) surface 240
 - AX_4 (CH_4 , CF_4 , SiCl_4) 154
 - AX_6E molecules 155 f.
 - AX_7 molecules 155 f.
- b**
- B_2H_6 145
 - back bonds 180
 - back-bonding 363
 - back-donation 363, 364
 - π -back-donation 352
 - basin populations 16, 154
 - basin volume 16, 297, 299
 - basins 142
 - basis set superposition error (BSSE) 460, 461
 - BCC *see* bonded charge concentration
 - BCP *see* bond critical point
 - Becke and Edgecombe 438
 - benzene 392, 393, 395, 403, 406, 408, 412
 - benzocyclobutadiene 408
 - m*-benzynes 392 ff.
 - BF_3 6 ff.
 - BH_3 368
 - bicyclo-[1.1.1]-pentane 98, 100, 101, 111, 116
 - bicyclo[3.3.1]nonane 115
 - bicycloalkane 99, 114, 116
 - binding energy 454
 - biphenylene 408
 - bond charges 72, 75, 80, 275
 - bond contribution 66 ff., 69 ff., 74, 92
 - to the energy-gradient-based force 85
 - bond critical point (BCP) 4, 10, 25, 141, 168, 231, 260, 271, 375, 426, 431 ff., 477
 - bond current contribution 89
 - bond ellipticity 12, 184, 185
 - bond force 85
 - bond order 11, 13, 15, 25, 135
 - bond path 4, 11, 52, 141, 232, 260, 386
 - connectivity 357
 - bond polarizability model 97
 - bond properties 11, 218
 - bonded charge concentration (BCCs) 182
 - bonded interactions 130
 - bonded radius 11
 - bond-length aberrations 334
 - bond-order model 425
 - borazine 407
 - Born–Oppenheimer energy surface 460
 - Born–Oppenheimer approximation 123
 - Born–Oppenheimer procedure 55
 - Bragg angle 285
 - branched alkane 114
 - BSSE *see* basis set superposition error
 - Buckingham-type potentials 437
 - buckminsterfullerene allotropes of carbon 208
 - buckybowls 409
 - bulk modulus 220, 221
 - 1,3-butadiene 418
 - butane 111, 115, 129, 194
 - 2-butanol 332
- c**
- C_2H_2 156
 - C_2H_2 dimer 129

- $(\text{C}_2\text{H}_2)_2$ 132
 C_2H_4 156
 C_2H_6 348
 CaF_2 216
 cage critical point 4, 5, 168, 388
 calculus of variations 41
 Carbo index of similarity 26, 487
 carbon monoxide 20, 21, 348, 445
 carbonyl supported metal–metal interactions 357
 Cash–Karp Runge–Kutta (CRRK) method 232
 catalytic activity 236
 catastrophe point 357
 CH bond 111
 CH stretching modes 96
 CH_4 103, 109
 characteristic set 4
 charge-assisted hydrogen bonds 199, 458
 charge concentrations 141
 charge-density refinement 308
 charge transfer 78, 176, 188, 431
 – contribution 73, 80
 – dipole 21
 – moments 176
 chemical structure 52
 chemical transferability 195
 chiral invariants 330
 chiral modules 336
 chirality 336
 chlorine 276
 chrysene 408
 ClF_3 155
 cisplatin 510
 Clar structure 417
 Clar's aromatic sextet 395, 416f.
 class I clathrates 189
 clathrate type I structure 187
 closed-shell bonding 8, 12
 closed-shell character 355, 445
 closed-shell interactions 11, 174, 260, 358, 427, 436, 441, 443
 clustering procedure 313
 CO *see* carbon monoxide
 $\text{CO}(\text{NH}_2)_2$ 264, 272
 CO_2 82
 $\text{CO}_2(\text{CO})_6(\text{ASH}_3)_2$ 352, 353
 $\text{CO}_2(\text{CO})_6(\text{NH}_3)_2$ 353
 $\text{CO}_2(\text{CO})_6(\text{PH}_3)_2$ 353
 $\text{CO}_2(\text{CO})_6(\text{XH}_3)_2$ 352
 $\text{CO}_2(\text{CO})_6(\mu\text{-CO})(\mu\text{-C}_4\text{H}_2\text{O}_2)$ 355
 $\text{CO}_2(\text{CO})_8$ 201, 369
 $[(\text{CO})_5\text{Cr-H-X}]^-$ 368
 $(\text{CO})_5\text{M}(\text{H}_2)$ 364
 commutator average 47
 compensatory transferability 56
 complementary ligands 488
 π -complexes 357 ff.
 π -complex–metallacycle 364
 compressibility 220, 221
 conditional pair density 10, 192
 conformational space 357
 connectivities 207
 contergan/thalidomide scandal 336
 CONTOR 29
 coordination 351
 coordinatively unsaturated sites (CUS) 236
 core basin 142
 core-valence bifurcation index 439
 correlation energy 276, 277
 correspondence rule 345
 Coulomb
 – correlation 14, 377
 – energy 123, 125, 134, 139
 – expansion 131
 – hole density 402
 – interaction 125, 129, 133
 coupling constants 375
 covalence degree (DC) 447
 covalent bonds 216, 354, 455
 CPHF method 80, 91, 106
 CPU time 129
 $\text{Cr}(\text{CO})_5$ 368
 $\text{Cr}(\text{CO})_5(\text{C}_2\text{H}_4)$ 363
 $\text{Cr}(\text{CO})_5(\text{H}_2)$ 364
 $\text{Cr}(\text{CO})_6$ 351
 $\text{Cr}(\text{PH}_3)_5(\text{H}_2)$ 364
 Cr–Cr path 367
 $[\text{Cr}_2(\mu_2\text{-H})(\text{CO})_{10}]^-$ 367
 crambin 288
 creation energy 247, 250
 critical points 2, 167, 209, 210
 $\text{CrOs}(\text{CO})_{10}$ M–M bonds 352
 CRRK *see* Cash–Karp Runge–Kutta
 CRYSTAL 27, 166, 167, 174, 223, 336
 – graphs 232
 – software 170
 – topologies 224
 CRYSTAL's LCAO 225
 crystalline isostructural families 214 ff.
 crystallization 175, 176, 179
 crystallographic *R*-factors 334, 337
 cubic perovskite SrTiO_3 270
 current density 64, 89, 93
 curvatures 3, 443
 cusp condition 262
 cyclic delocalization 404
 cycloalkane 99, 114, 116

- cyclohexa-1,3-diene 408
 cyclohexa-1,4-diene 408
 cyclohexane 98, 101, 111, 113, 115, 408
 cyclohexene 408
 cytosine 415
- d**
- Dalton's atomic hypothesis 39
 dangling bonds (DBs) 180
 database of protein fragment contents 313
 dative bond 350 ff.
 DB *see* dangling bonds
 DC *see* covalence degree
 DCBS *see* dimer-centered basis set
 DCD *see* Dewar–Chatt–Duncanson
 Debye–Waller factor 286
 deformation density 172, 173
 – maps 354
 delocalization 9, 13–15, 351, 375
 π -delocalization 407
 delocalization index 13–15, 135, 166, 167,
 201, 347, 351, 355, 363, 375, 377, 378, 391,
 395, 402, 405, 407, 460
 density of states (DOS) 187
 depletions 141
 Dewar structure 403
 Dewar–Chatt–Duncanson (DCD)
 – donor–acceptor complexes 357, 361,
 363
 – ring complex 359
 – mechanism 351
 – model 364
 DI *see* delocalization index
 diagonalized quadrupole tensor 24
 diamagnetic spin–orbit interactions 378
 diamond 208, 216, 219
 dielectric polarization 20
 Diels–Adler reaction 409, 418 f.
 1,12-difluoro[4]helicenes 5, 6
 diffuseness *D* 183
 dihydrogen bond 426, 456
 dihydrogen bonding 8
 dihydrogen complexes 364
 dimer-centered basis set (DCBS) 460
 dimethylcyclobutane 115
 dimethyl-phosphinoyl (methylsulfonyl)
 methane 390
 dipeptide L-phenylalanyl–L-proline H₂O 318
 dipole derivative 80
 dipole moment 21, 22
 – derivatives of CO₂ 81
 dipole polarizability tensor 74
 Dirac–Slater exchange density 272
 diradicals 393
 dispersion energy 459
 dissociation energy 436, 439, 440
 disynaptic basins 145, 438
 DL-serine 329, 334
 DMACB 170, 171
 DMSDA *see* mean-square displacement
 amplitudes
 DNA bases 25
 docking applications 314
 domain-averaged Fermi hole 487
 σ -donation 352
 donor–acceptor bond 350
 donor–acceptor interaction 352
 DOS *see* density of states
 Drude model 215
- e**
- ECP *see* effective core potential
 EF *see* eigenvector following
 effective core potential (ECP) 27
 Ehrenfest
 – force 53, 64, 260, 381
 – theorem 52
 eigenvector following (EF) 168
 electric dipole derivative 80
 electric dipole moment 68, 71
 electric dipole polarization 61
 electric field 78, 109, 110
 – derivative 73, 75
 – flux 63
 electric polarizability 68, 73 ff., 90
 – tensor 76
 electric susceptibility 50
 electron delocalization 13–15, 376, 382, 385,
 395, 399, 400–401
 electron isodensity maps 391
 electron localization 9, 14, 128, 143, 401,
 440
 electron localization function (ELF) 142 ff.,
 191, 277, 438
 electron pair localization 347
 electron transfer 431
 electron tunneling microscope 54
 electronegativity 20, 150, 215, 294, 218, 313,
 311, 484
 electronic current density 90
 electronic energy of an atom in a molecule
 82
 electronic pressure density 83
 electronic structure of molecules 54
 electrophile attack 249
 electrostatic force 86
 – on a nucleus 87
 electrostatic interaction energies 312, 313

- electrostatic model 351
 electrostatic moments 20–25, 138, 139
 electrostatic potential 249, 311, 400, 475, 482
 electrostatic properties 287, 289, 305 ff.
 – of a protein site 313
 electrostatic–covalent hydrogen bond model 459
 ELF *see* electron localization function
 – ELF basins 149 ff.
 – ELF population analysis 147 ff.
 – ELF topology 144 ff.
 – ELF valence basin 166, 200
 ellipticity 12
 elpasolites 214
 energy density 12 ff., 272
 energy derivatives 84
 energy-gradient-based force 64, 65, 86
 – on the nucleus 83
 enzymes 511
 estrone hormone 15
 ethane 98, 109, 112, 113, 194, 379, 380, 418
 ethanol 332
 ethene 98, 111
 ethyne 98, 111
 Euler equation 41
 Euler's invariant formula 211
 exact exchange energies 133
 exact exchange force 127
 EXAFS *see* X-ray absorption fine structure
 exchange between electrons of the same spin 272
 exchange correlation 377
 exchange density 274
 exchange eigenvalues 138
 exchange energy 122, 124, 125, 127, 128, 130 ff., 136, 276, 277
 exchange force 136, 137
 exchange interaction 131
 exchange interaction energy 461
 exchange moments 126, 139
 exchange potential 278
 exchange–correlation density 401, 402
 exchange–correlation energy 271
 expectation value of an operator 9
 experimental electron density 261
 experimental H \cdots O interactions 436
 external magnetic field 89
 external potential 474
 EXTREME 27
- f**
- F₂ 445
 F-center in sodium electrosodalite 190
 F-center basins 192
 F-centers 186
 Fe–Fe bonding 369
 Fermi
 – contact 378
 – contact contribution 379
 – – to ${}^3J_{\text{HH}}$ 378
 – correlation 14
 – hole 144, 167, 375, 377, 378, 402, 403, 487
 – level 189
 ferromagnetic phase of SES 191
 Feynman path–integral method 271
 Feynman
 – force 52, 381
 – theorem 52
 F–F coupling constants 380
 F \cdots H hydrogen bonded complexes 441
 [F \cdots H \cdots F][–] system 444
 F–H $\cdots\pi$ hydrogen bond path 456
 FH \cdots ClH 146
 (FH)₂ 420, 437
 first atomic electrostatic moment 20
 first derivative of the electric dipole moment 78
 first-order reduced density matrix 123
 Fisher information 144
 fixed nucleus approximation 55
 flatness 354
 π -fluctuation aromaticity index (FLU $_{\pi}$) 406 ff., 415, 419, 420
 flux through a surface 47
 force fields 26, 121
 formamide 333
 formic acid–formate anion complex 199
 Fourier
 – difference synthesis 225
 – transformation 289
 fpLAPW *see* full potential linearized plane wave
 FRAGDIP 21
 fragment charges 312
 fragment deformation maps 354
 fragment electroneutrality 307
 fragment representations 313
 fragment transferability 338
 free electron gas 215
 Fukui
 – frontier orbital theory 54
 – functions 475
 – Nobel Lecture XXI
 – radical reactivity indices 484
 full potential linearized augmented plane wave (fpLAPW) formalism 223

- fullerenes 319, 409
Fulton bound index 391
- g**
GAMESS 27, 29, 128
gauche effect 383
Gauss's theorem 18
Gaussian 27, 29, 30, 106, 114 ff., 332
Gaussian 03 129
Gaussian 94 295
genetic code 22–24, 26
GFMLX 336
GIAO 413
globbic structure factors 289
glycine 124
goodness of fit 334
gradient kinetic energy 17
gradient path 242, 428, 474
gradient vector 6
– field 6, 142, 259, 323
– field lines 211
– instability 210
gradient-corrected correlation energy 275
gradient-corrected energy density 272
gradient-corrected exchange density 274
graphite 208, 219
GRDVEC 28, 29
Green's function 192, 263, 271
GRIDV 28, 29
group additivity schemes 82
group contribution 22, 50
– to the polarizability tensors 77
guanine 415, 416
guanine–cytosine base pair 415
guest atoms 188
guest–host binding energy 189
guest–host systems 165 ff.
– binding energy 189
- h**
 $\text{H}_2\text{N}-\text{C}_x\text{H}_2(\text{R})-\text{COOH}$ 21–23, 295
 $\text{H}_3\text{N}\cdots\text{HF}$ 439
 H_2O dimer 129
Hamiltonian approach to quantum mechanics 38
Hammitt substituent constants 412
Hansen–Coppens XXII
– multipole model 261, 262, 318
hAR *see* human aldose reductase
harmonic approximation 78
harmonic oscillator model of aromaticity (HOMA) 394, 400, 404, 406 ff., 410, 412 ff., 420
Hartree–Fock
– energy 123
– virial 29–30
– wave functions 127
Hattig's recurrence formulae 129
HB *see* hydrogen bond
HCCH \cdots HF complex 456
HCN 445
HCH \cdots O intermolecular interactions 170
HDN *see* hydrodenitrogenation
HDS *see* hydrodesulfurization
heats of formation 50
heavy main-group element 352
hedrane 114, 116
Heisenberg
– equation of motion 37
– representation of quantum mechanics 51
Hellman–Feynman
– electrostatic force 19, 65, 83
– electrostatic theorem 83, 85, 87, 88
Hermitian operator, linear 46
Hermiticity 47
Hessian matrix 3, 231, 427
hexaprismane 117
1,3,5-hexatriene 129, 134
HF dimer 129, 130
H \cdots F hydrogen-bonding interactions 437
H \cdots H bonding 8, 9, 11
H \cdots H electrostatic interaction 445
hierarchical merging/clustering algorithm 292, 301
higher-order polarizability 104
high-pressure phosphorous boride 215
high-resolution
– electrostatic potentials 306, 308, 309
– protein model 287
Hirshfeld
– multipole model 262
– test 318, 335
H \cdots N hydrogen-bonding interactions 441
(H_2O)₂ 131, 132, 430
H \cdots O hydrogen bonds 436
H \cdots O interactions 437
Hohenberg–Kohn
– formulation of DFT 261
– theorem XX, 474, 475
HOMA *see* harmonic oscillator model of aromaticity
homodesmotic reaction 400
homogeneous electron gas 263
homoleptic $\text{M}_2(\text{CO})_n$ dimers 352
host–guest
– chemistry 186
– systems 186 ff.

- human aldose reductase (hAR) 287 ff.,
291 ff., 300
– crystal structure 299
– structure 307, 312, 313
- hybrid orbital-free energy functionals 271
- hydride bond 466
- hydride bridges 367 ff.
- hydrides 153
- hydrodenitrogenation (HDN) 236
- hydrodesulfurization (HDS) 236, 237
- hydrogen bond(ing) (HB) 170, 177, 197,
199, 217, 273, 331, 416, 425, 427, 429, 453
– Coulomb interaction 130
– donor 504
– energies 454
– exchange energy 132
– intermolecular 453
– molecular complexes 198
- hydrogen–hydrogen bonding 8
- hydroimidazo[4,5-*d*]imidazole 430
- hydrophilic regions 500
- hydrophobic effects 481
- hydrophobic regions 500
- hydrophobic–hydrophilic interaction tendency
483
- hydrophobicity 483
- hydroxy-2-aminopurine 508 (6-)
- hyperconjugation 386
- hyperpolarizability 61, 73
- hypervirial theorem 83, 86
- hyperwall mode 505
- i**
- I₂O 216
- IAM *see* independent atom model
- ice VIII 436
- iceane *see* tetracyclo-[5.3.1.1^{2,6}.0^{4,9}]-
dodecane
- independent atom model (IAM) 172, 174,
189, 286 f., 329, 334, 336
- independent transferability 113
- induced electronic magnetic dipole moments
88 f.
- influence function 192
- infrared intensity 50
- infrared spectrum 78
- infrared vibrational absorption intensity 68
- inhibitor–protein interactions 286
- inner-valence shell charge concentration
(i-VSCC) 509 ff.
- inorganic clathrates 186
- integrated atomic electronic energy 277
- integration error 18, 276
- intensity of absorption 78
- interaction
– density 261
– energy 435
– energy-decomposition scheme 459
– potential 436
– tensor 127
- interatomic surface (IAS) 8, 11, 63, 244,
232, 377, 426, 477
- intermolecular interaction 131, 435
- invariom 317, 331, 334
– aspherical scattering factors 329
– database 330, 336
– pseudoatoms density 338
- inverse hydrogen bonding 466
- inverse moments 122
- ionic bonds 217
- ionic character 151
- ionic contributions 151
- ionicity 216
- isobutane 99
- isodensity envelope 17
- isopropanol 332
- isotropic polarizability 77
- k**
- Karplus-type behavior 379, 382
– of ³J_{HH} 395
- Kekulé
– resonance structure 416
– structures 403
- Kenichi Fukui XXI
- kinetic energy 43 f., 122, 123, 266
– density 12, 13, 18, 37, 259, 262 ff.,
349, 354, 381, 391, 432, 482, 483
– operator 17
– per electron 192
- Kohn–Sham
– approximation 378
– density-functional theory 128
– exchange-correlation energy 128
– orbitals 128
- l**
- Lagrange polynomial interpolation 232
- Lagrangian
– action principle 37
– classical 41
– equation of motion 41
– representation of quantum mechanics
51
- L-alanine 208
- Laplacian of the electron density 3, 10, 17,
44, 141, 149 f., 177, 182, 192, 200, 215, 218,

- Laplacian of the electron density (cont.)
 259, 262, 324, 346, 363, 427, 445, 458, 483,
 488, 500 ff.
- LBHB *see* low-barrier hydrogen bonds
- Le Chatelier principle 56
- Leu–Enkephalin 294
- Lewis, G. N. 502
 – acid 10, 252, 253, 466
 – acidity VSCCs 367
 – base 10, 466
 – model 145, 345, 352, 378, 438
 – structures 157
- LFT *see* ligand-field theory
- Li 216
- LiC≡CLi...HF complex 456
- LI-DICALC 28
- LIF 269, 270
- ligand–protein interactions 286
- ligand-field theory (LFT) 349, 352
- limits of transferability 331
- local aromaticity criteria 413
- local bulk moduli 220, 221
- local dipole moment 96
- local electron affinity 484
- local electronic charge concentration 10
- local energy densities 443
- local exchange energy 273
- local hardness 484
- local polarizability 484
- local source (LS) 192, 194
- local statement of the virial theorem XX, 13,
 56, 346
- localization
 – domains 145 ff., 156
 – function 142
 – indices 14, 15, 167, 377
 – nodes 146
 – tree-diagram of H₂CO 147
 – tree-diagram of NaCl 147
- lock and key mechanism 352
- lone pair 145, 438
 – electron concentrations 275
- Lorentzian form 144
- low-barrier hydrogen bonds (LBHB) 446
- low-electronegativity elements 214
- low-pressure boron phosphide 215
- LS *see* local source
- m**
- M...CO interactions 352
- M₂(CO)_n 356
- macromolecular crystallography 285
- magnetic dipole moment 88
- magnetic susceptibility 50
- magnetizability 64, 68, 90
 – tensor of naphthalene 92
- malonaldehyde 199
- matrix of exchange moments 136 ff.
- maximum entropy method (MEM) 187, 188
- M–C interactions 370
- mean molecular polarizability 97, 98
- mean-path approximation 271
- mean-square displacement amplitudes
 (DMSDA) 335
- measurable properties 50
- medium-resolution electrostatic potential
 310
- MEM *see* maximum entropy method
- metallacycles 357
- metal–metal (M–M) bond(ing) 199, 349, 352,
 354 ff., 370
 – bond path 354, 369
 – contacts 352
 – interactions 354, 370
- metal–olefin complexes 361
- methane 107, 109, 113
- methanol 332
- methyl fluoride 509
- methyl group 77, 195
- N-methylacetamide 333
- methylcycloalkanes 99
- methylcyclobutane 115
- N-methylformamide 333
- methylcyclopropane 115
- methylene group 56, 109
- misdirected valence 511
- Mn...CO intramolecular interactions 356
- Mn₂(CO)₁₀ 201, 355
- Mn–Mn bond 200, 201, 355
- molar volumes 50
- molecular complexes 196 ff.
- molecular crystals 170 ff.
- molecular devices 55
- molecular dipole 170, 176
- molecular electrostatic potentials 313
- molecular expectation value 10
- molecular graph 8, 52
- molecular orbital theory 54
- molecular polarizability 73, 77, 96 ff., 99,
 109, 110, 113
- molecular potential 122
- molecular quantum similarity measures
 (MQSM) 487
- molecular response properties 61
- molecular similarity 26
- molecular structure stability 52
- molecular virial theorem XX, 29, 86, 88
- molecular volume 481

- molecular graph 5
 Møller–Plesset perturbation theory 29
 monopolar exchange moment 128
 monosynaptic basins 145, 438
 MORPHY 27, 332
 – 01 128, 129
 Morse equation (relationship) 4, 168, 172
 Morse-type potentials 437
 Mo–S
 – bond 242, 244, 246
 – inter-atomic surfaces 246
 MoS₂ 239, 245 ff.
 – bulk 241 ff., 244
 – unit cell 241
 MQSM *see* molecular quantum similarity measures
 mRNA codon 22–24
 muffin tins 223
 multiple bonds 156 ff.
 multiple-exchange energies 133
 multipolar database library 287, 306, 307, 309
 multipolar ED database fragment 287
 multipolar refinement technique XXII
 multipole expansion 130 ff., 137
 multipole model 264, 277, 336
 multipole moments 121
- n**
 N...N contacts 172
 N₂ 216
 N₂...HF 439
 NaCl 146
 NADP⁺ 293, 302, 312
 NaF 348
 nanotechnology 55
 naphthalene 91, 93, 392 ff., 408
 naphthacene 408
 natural bond orbital (NBO) 446
 natural coordinates 104
 natural orbitals 378
 NBM *see* non-bonded maxima
 NBO *see* natural bond orbital
 Ne₂ 348
 nearest-neighbor approximation (NNA) 333
 negative hyperconjugation 364
 net current vector 64
 neural networks 121
 Newton's equation of motion 41
 Newton–Raphson (NR) technique 168, 231, 236
 N...H hydrogen-bonding 433
 N–H...N hydrogen bonds 172, 446
 – complexes 441
 N–H...O hydrogen bonds 172, 448, 462
 NICS *see* nucleus-independent chemical shift
 NiMoS 239, 240
 Ni–Ni interaction 354
 NMR shielding tensors 90
 N–N
 – bond 217
 – contacts 171, 172
 NNA *see* non-nuclear attractors *and* nearest-neighbor approximation
 non-bonded charge concentration (NBCC) 182
 non-bonded interactions 130
 non-bonded maxima (NBM) 177, 178
 non-nuclear attractors (NNA) 6, 168, 191–193, 208, 314
 non-nuclear maxima (NNM) 6, 216, 218, 314, 225, 226
 non-stationary point geometry 62, 83, 84
 normal mode vibration 80
 normalized spherical harmonics 126
 normal-mode vibrational coordinates 79, 80
 NR *see* Newton–Raphson
 N-representability problem 378
 nuclear critical points 2, 4, 168
 nuclear momentum operator 86
 nuclear virial energy 62, 68, 83, 86
 nucleophilic attack 249, 250
 nucleus-independent chemical shift (NICS) 400–420
 null (zero value) molecular property 61, 62, 64, 66, 70
 numerical integration error 29
- o**
 observables 16
 occupation numbers 378
 octet rule 155
 OH fragment transferability 332
 O–H...O hydrogen bond 448, 462
 oligopeptide molecules 336 ff.
 one-electron density matrix 56, 123, 166, 260, 263
 open quantum system 44
 open-shell character 355
 orbital conservation 54
 orbital models 54
 ORCRIT 289, 290
 origin-dependent atomic charge-transfer dipole contribution 72
 origin-dependent atomic contributions 61, 68, 87
 origin-dependent atomic property 85

- origin-dependent charge transfer term 62
 origin-dependent polarization term 62
 origin-independent atomic contribution 61
 origin-independent property density 61
 overlap function at a point 125
- p**
- packing forces 368
 PAH *see* polycyclic hydrocarbon
 pair density 166, 376
 – functions 376
para-delocalization index (PDI) 404 ff., 410,
 414, 415, 417
 paramagnetic spin–orbit 378
para-nitroaniline 71 ff., 74, 76 ff.
 PASA *see* promolecular atom shell
 approximation
 path integral approach 49
 Pauli
 – exclusion principle 377
 – repulsion 144, 381, 438
 PBH *see* polybenzenoid hydrocarbons
 PCl₅ 155
 PDI *see* *para*-delocalization index
 penamcillin 499, 504
 penicillin 506, 507
 – derivative 504
n-pentacosane 114
 pentadecane 114
 pentane 111, 113, 115, 194
 peptide
 – bond 328
 – crystals 297
 – HN–H_xC_x–C=O group 299
 – plane HN–H_xC_x–C=O 294
 pericyclic concerted reaction 418
 periodic systems 231
 perovskites 214
 pharmacophores 499
 phenanthrene 8, 392 ff., 408, 416
 phenol 332
 p*K*_a of weak acid 26
 Poincaré–Hopf formula (relationship) 4,
 6 f., 66, 209
 point-charge models 122
 polar bonds 215, 455
 polarizability 64, 78, 80, 110, 111, 400, 483
 – tensor 11103
 polybenzenoid hydrocarbons (PBHs) 391,
 393, 394
 – aromatic dilution 394
 polycyclic aromatic hydrocarbons (PAHs)
 404, 409, 410, 416, 417
 polymorphism 208
 polysynaptic basins 438
 population analysis 145
 porphyrin 288
 post Hartree–Fock wave functions 27–30,
 127
 potential energy density 8, 12, 25, 56, 259,
 262 ff., 349, 354, 381, 462
 powerwall mode 505
 primary bundle 211, 212
 principle
 – of least action 38
 – of stationary action 47, 49
 PROAIM 27, 29, 193, 477
 procrystal 267
 PROMEGA 193
 promolecular atom shell approximation
 (PASA) 290
 promolecular model 217, 222
 promolecule maps 300
 propane 98, 109 ff., 194
 propellane 99, 114
 proper open quantum system 7, 8, 50
 proper operator 50
 properties after molecular reconstruction
 481
 protein
 – binding site 313
 – crystal structures 285
 – crystallography 285
 – electrostatic properties 287
 – main chain HN–C=O peptide plane
 288
 – molecules 336 ff.
 – refinement 289
 – retention time 26
 – stability 26
 – structure 289, 311
 protein–DNA docking 290
 protein–ligand interaction energies 289
 protein–protein docking 290
 protein–protein interaction energies 289
 proton–proton vicinal coupling constants
 380
 pseudoatom 7, 275, 329
 – fragments 317
 pseudoatomic density 261
 pseudopotential 169, 222
 pyracelene 408
 pyridine 406, 408
 pyrimidine 408
- q**
- QTAMC *see* quantum theory of atoms in
 molecules and crystals

- quadrupole moment 24
 quality of an atomic integration 18
 quantitative structure–activity/property relationship 473
 quantum
 – observables 37
 – self-similarity measure 487
 – stress tensor density 51
 – vector current density 51
 quantum theory of atoms in molecules and crystals (QTAMC) 259, 272
 quinoline 408
- r**
 radial density functions 261
 radius concept 207
 Raman
 – scattering intensity 95, 97 ff., 103 ff.
 – spectroscopy 95
 rank 4
 reciprocal space vectors 289
 RECON 476 ff.
 reduced density matrices 121
 reference density 188
 regularity in the genetic code 24
 Reiss–Münch theorem 475
 relative hardness 400
 relativistic effects 55
 relief map of the electron density 2
 residual electron density 318, 337
 resonance structures 416
 resonance-assisted hydrogen bonds 457, 458
 response properties 62
 R-factor 336
 ring
 – critical point (CP) 4, 5, 168, 388
 – currents 399
 – strain 5
 – surface 5
 rotational barriers 375
- s**
 scanning tunneling microscopy (STM) 237
 Schrock carbene 512
 Schrödinger's
 – functional 46
 – kinetic energy 17
 – time dependent equation 41
 Schwinger's principle of stationary action 8, 46, 50, 476
 scorpion toxin 288
 SCVS *see* self-consistent virial scaling
 SD *see* softening degree
 second atomic electrostatic moment 24
 second-order (pair) density 401
 second-order density matrix 14
 second-order Jahn–Teller symmetry rule 54
 self-consistent virial scaling (SCVS) 30, 85, 86
 self-interaction 124
 separability 394 (σ – π)
 SES *see* sodium electrosodalite
 SF₄ 155
 SF₆ 155
 shared-shell
 – character 445
 – interactions 174, 441, 443
 sharing of electrons 13
 shell structure 346
 SHELXL 336
 short strong hydrogen bond (SSHB) 463
 Si crystal 225, 226
 Si(111)(1 × 1) 180 ff., 184
 Si(111)(1 × 1)–H 181
 – surface 180
 Si(111)(2 × 1) 180
 – reconstructed surface 184 ff.
 – surface 185
 Si₂Me₂ 157
 Si₂Me₄ 157
 side-chain fragments 308
 signature 4
 silanes 114, 117 f.
 silicon bulk 182
 similarity index 26, 488
 single-enantiomer drugs 336
 singlet diradicals 393
 Si–O bonds in silicates 436
 Si–Si bond properties 180
 slab model 180, 181
 sodium electrosodalite (SES) 186, 190 ff.
 softening degree (SD) 447
 solid peoperties 207
 source contribution 198, 201
 source function 165, 192 ff., 196 ff., 201 f.
 spherical harmonics 125
 spin density 148, 190, 191
 spin population 16, 143
 spin–dipolar interactions 378
 spin-independent electron correlation 272
 spin-less pair density 401
 S–S
 – bond 242, 251, 427
 – bond critical points 242, 245
 – bond paths 242
 – interatomic surface 253
 SSHB *see* short strong hydrogen bond
 stability of gradient vector field 53

- π - π stacking interaction 25
 - STM *see* scanning tunneling microscopy
 - stress tensor 64
 - strong hydrogen bonds 455
 - strong van der Waal's covalent interactions 440
 - structural stability 52, 53
 - substituent effects 412
 - supramolecular chemistry 186
 - surface
 - contribution 46
 - derivatives 75
 - flux 47
 - layer 182
 - terms 46
 - symmetry-stabilized agostic interaction 368
 - synaptic order 145, 166, 438
 - synchrotron radiation 318 ff.
- t**
- TAE *see* transferable atom equivalent
 - tert*-butylcyclohexane 391
 - tetalin 392
 - tetracyclene 99
 - tetracyclo-[5.3.1.1^{2,6}.0^{4,9}]-dodecane (iceane) 115
 - tetrahydroimidazol[4,5-*d*]imidazole 429
 - tetralin 395
 - thermodynamic property 208
 - of ice VIII 437
 - partitioning 220
 - Thomas-Fermi
 - approximation 263
 - kinetic energy functional 438
 - three-center (3c) systems 357
 - three-center bonding 356 ff.
 - TiCl₃(C₂H₅) 366
 - time-independent electric field 74
 - TMS *see* transition metal sulfides
 - topological atoms 123, 129
 - topological multipole expansion 122
 - topological polymorphism 215
 - topological polytypism 208, 214, 215
 - topological properties 376
 - TOPOND 27, 165 ff., 170
 - TOPXD 168 ff.
 - total energy 123
 - total energy density 346, 432
 - total molecular volume 178
 - total polarization contribution 73
 - transferability 55, 56, 82, 111, 194, 287, 294, 297 f., 317, 324, 327, 331, 332, 504
 - transferable atom equivalent (TAE) 474 ff., 513
 - transferable methylene contribution 77
 - transferable multipolar data 289
 - transition metal sulfides (TMS) 236
 - transition probability 26
 - transition metal
 - atoms 509 ff.
 - carbonyl complexes 351
 - ions 511
 - triazine 408
 - triphenylene 408
 - trisynaptic basins 145, 438
 - TS *see* aromatic transition state
 - two-center bonding 349 ff.
 - two-center-two-electron (2c-2e) bonds 349
 - two-electron density matrix 166, 260
 - tyrosine 22, 24, 294, 299
 - tyrosine-glycine peptide bond 294
- u**
- uniform electron gas 272
 - unsaturated hydrocarbons 117 f.
 - urea 171 ff., 264 ff.
 - crystal 171, 177
- v**
- valence basin 142, 438
 - populations 149
 - valence flatness 315
 - valence shell charge concentration (VSCC) 149, 177, 182, 347, 349, 350, 355, 502
 - valence shell charge depletion (VSCD) 502, 508
 - valence shell electron pair repulsion (VSEPR) model 141, 149, 150, 153 ff., 157, 158, 378, 511
 - electron domains 149 ff.
 - van der Waals
 - bonds in graphite 219
 - complexes 454
 - interactions 455
 - repulsion 383
 - variation of the surface 45
 - vibrational frequency 84, 96
 - vibrational modes 96
 - vibrational spectra 79
 - virial 30
 - virial field 12, 56
 - virial graph 8
 - virial of the electronic Ehrenfest force 83
 - virial operator 83
 - virial path 8, 9, 260
 - virial ratio 20, 29
 - virial theorem XX, 20, 29, 37, 52, 85, 260, 271, 432

- virtual high-throughput screening 473
 vitamin B₁₂ 320, 321, 323
 VmoPro 307, 309, 311
 volume rendering 500
 volumes 150, 178
 von Weizsäcker kinetic energy functionals 438
 VSCC *see* valence shell charge concentrations
 VSCD *see* valence shell charge depletion
 VSEPR *see* valence shell electron pair repulsion
- W**
- W(CO)₃(PR₃)₂(H₂) 364
 Walter Kohn XXII
 water 276
 water dimer 137, 138, 199
 Watson–Crick base pair 415
 wavefunction 27, 42, 85
 weak hydrogen bonds 455
 weak interactions 441
- weak van der Waal's covalent interactions 440
 WIEN 223
 WIEN's fpLAPW 225
- X**
- XD 165, 168, 169
 X–H···F–Y complexes 443, 444
 X–H···O hydrogen-bonding interactions in crystals 436
 X–H···Y hydrogen bonds 499
 (XH₃)(CO)₃Co–Co(CO)₃(XH₃) molecules 355
 X-ray absorption fine structure (EXAFS) 236
 XTAL 289, 290, 298, 300, 303
- Z**
- zero flux
 - condition 6, 9, 17, 44, 46, 275
 - surface 6, 9, 10, 44, 48, 323, 354, 426, 429

